Energy & Environmental Science

Accepted Manuscript

ROYAL SOCIETY OF CHEMISTRY

www.rsc.org/ees

Broader context

The conversion of methane into methanol is very difficult chemistry requiring catalysts operating at elevated temperatures and pressures. The prospects of a future methanol economy depend on successful development of robust and efficient catalysts that can accomplish this chemistry under mild conditions. In nature, the particulate methane monooxygenase (pMMO), a membrane-bound metalloenzyme, catalyzes methane oxidation with total selectivity and atom efficiency. Inspired by what we have learned about the pMMO over the past two decades, a tricopper complex based on the catalytic site of this enzyme has been developed and shown to mediate methane oxidation to methanol selectively. However, as a homogeneous catalyst, the catalytic efficiency is low because of the low solubility of methane in the solvent supporting the catalyst. Here, we describe the immobilization of the tricopper catalyst into mesoporous silica nanoparticles (MSN) to take advantage of the "over solubility" of methane in liquids confined in nanoporous materials relative to the bulk solubility. This heterogeneous formulation of the tricopper cluster is capable of converting methane into methanol with high catalytic efficiency and excellent product yields without over-oxidation at room temperature. The heterogeneous catalyst is also robust and reuseable.

Heterogeneous formulation of the tricopper complex for efficient catalytic conversion of methane into methanol under ambient temperature and pressure†

Chih-Cheng Liu,[ab] Chung-Yuan Mou,[a] Steve S.-F. Yu,[b] and Sunney I. Chan*[ab]

[a] *Department of Chemistry, National Taiwan University, Taipei 10617, Taiwan. Email: cymou@ntu.edu.tw; d98223115@ntu.edu.tw*

[b] *Institute of Chemistry, Academia Sinica, Nankang, Taipei 11529, Taiwan. Email: sfyu@gate.sinica,edu.tw; sunneychan@yahoo.com*

† Electronic supplementary information (ESI) available. See DOI:

Abstract

The development of a heterogeneous catalyst capable of efficient selective conversion of methane into methanol with multiple turnovers under ambient conditions is reported here. The catalyst is assembled by immobilizing into mesoporous silica nanoparticles the tricopper complex $[Cu^{I}Cu^{I}Cu^{I}(\mathbf{7\text{-}N\text{-}Etppz})]^{1+}$, where **7-N-Etppz** stands for the organic ligand 3,3'-(1,4-diazepane-1,4-diyl)bis[1-(4-ethylpiperazine-1-yl)propan-2-ol]. This tricopper cluster complex has been previously shown to mediate efficient methane oxidation without over-oxidation in homogeneous solution when the catalytic turnover is driven by hydrogen peroxide in acetonitrile. The turnover mechanism of the catalyst is similar between the two formulations. However, the heterogeneous formulation exhibits

dramatically higher catalytic efficiencies and turnover numbers, with commensurate improvements in chemical yields, offering the most proficient catalyst for selective conversion of methane into methanol at room temperature developed to date. To explain the efficient methane oxidation, the over-solubility of nonpolar gases, such as methane, in liquids confined in nanoporous solids is evoked. The much higher solubility of methane within the pores of the mesoporous silica nanoparticles, as compared to the bulk solubility, led to very efficient turnover of the concentrated confined methane. This success underscores the advantages of using nanoparticles to support chemical catalysts for this difficult chemical transformation under these conditions.

Introduction

Successful development of a robust heterogeneous catalyst capable of mediating efficient methane (CH_4) oxidation to methanol (CH_3OH) and other components of natural gas to their corresponding alcohols will be a major step toward replacing petroleum as the source of chemical feedstocks in the chemical industry.[1] This advance will ultimately lead to an economy based on CH_3OH [2,3] and hydrogen[4] instead of petroleum. New methods will be developed for the manufacturing of fuels, fine chemicals, fibers, plastics, advanced materials, pharmaceuticals, and foodstuff that will be greener and energy more efficient with lower carbon footprint on the environment.[5] This will revitalize the chemical industry globally, creating intellectual opportunities for new science and technologies, and employment for young scientists in many fields, especially in chemistry, chemical engineering, biotechnology, *etc*.

Future of the CH_3OH economy rests on the development of inexpensive catalysts and energy-efficient and green processes for the direct oxidative conversion of CH_4 into CH_3OH to take advantage of the huge deposits of CH_4 on Earth.[6,7] In recent years, there have been a number of attempts directed toward developing a catalyst for selective CH_4 oxidation. These include platinum catalysts,[1,8-10] a mercury-catalyzed sulfuric acid system,[11] Cu-based zeolites,[12-15] Fe-ZSM-5[16] and Cu-Fe-ZSM-5,[17,18] Cu-mordenites,[19-23] among others.[24,25] Recently, we have also developed a homogeneous catalyst for CH_4 oxidation based on the tricopper cluster complex $[Cu^ICu^ICu^I(\mathbf{7\text{-}N\text{-}Etppz})]^{1+}$, where **7-N-Etppz** stands for the organic ligand 3,3'-(1,4-diazepane-1,4-diyl)bis[1-(4-ethylpiperazine-1-yl)propan-2-ol] (Scheme 1).[26,27] This tricopper complex is capable of efficient conversion of CH_4 into CH_3OH upon activation by dioxygen (O_2) without over-oxidation under ambient conditions. This development is significant as the design is based on our understanding of the catalytic site in the particulate methane monooxygenase (pMMO) from the methanotroph *Methylococcus capsulatus* (Bath), the most efficient CH_4 oxidizer discovered to date.[28-32] A recent study on tricopper-oxo clusters stabilized in copper-exchanged zeolites has also demonstrated the efficacy of the trinuclear copper system toward CH_4 oxidation.[23]

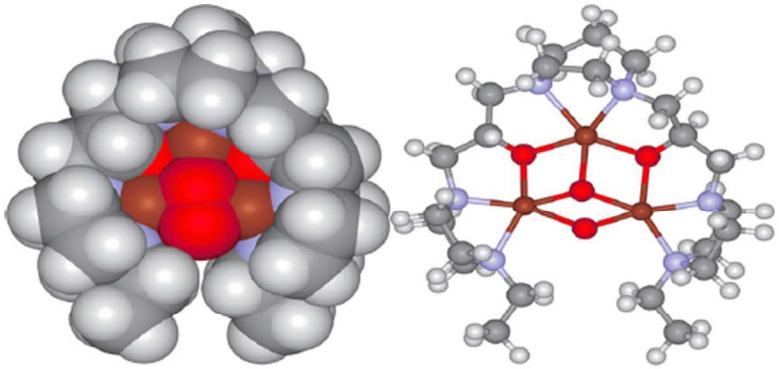

Scheme 1. Space-filling model (*left*) and ball-and-stick model (*right*) of the optimized structure of $[Cu^{II}Cu^{II}(\mu\text{-}O)_2Cu^{III}(\textbf{7-N-Etppz})]^{1+}$ showing the funnel-like opening or cleft at the bottom for a CH_4 substrate molecule to access the "hot" oxene group harnessed. H, white; C, gray; N, blue; O, red; and Cu, brown. Taken from Reference 26, Fig. 3.

The catalytic cycle for the $[Cu^{I}Cu^{I}Cu^{I}(\textbf{7-N-Etppz})]^{1+}$ catalyst is depicted in Scheme 2. To initiate the catalysis, the fully reduced tricopper complex is first activated by O_2 to form the highly reactive $[Cu^{II}Cu^{II}(\mu\text{-}O)_2Cu^{III}(\textbf{7-N-Etppz})]^{1+}$ intermediate harnessing the ""hot" oxene group in acetonitrile (MeCN).[26,27,30,31] The activation of the tricopper complex by O_2 and the transfer of one of O-atoms to an organic substrate, with the remaining O-atom embedded in the tricopper complex, has been confirmed by $^{18}O_2$ experiments.[33] When a CH_4 molecule becomes associated with the hydrophobic substrate-binding cleft at the base of the tricopper complex, the activated tricopper cluster can mediate facile O-atom transfer to one of the C−H bonds in the transition state (Scheme 2, *upper* panel).[26] This binding pocket is selective to small straight-chain alkanes from C1−C6.[27] Moreover, no over-oxidation is observed for CH_4, ethane and propane, underscoring the importance of selectivity in the controlled oxidation of these alkanes.[27] To regenerate the catalyst, the "spent" catalyst, namely, the $[Cu^{I}Cu^{II}(\mu\text{-}O)Cu^{II}(\textbf{7-N-Etppz})]^{1+}$ species, is reduced by one molecule of hydrogen peroxide (H_2O_2) to produce O_2 and H_2O. Note that the H_2O_2 is acting as a reductant in the turnover cycle, not the oxidant, which is O_2.[30,31] Thus, the catalyst is functioning as a methane monooxygenase, just like the pMMO enzyme, and one molecule of CH_3OH is produced per molecule of H_2O_2 consumed. Interestingly, although the catalyst is activated by O_2, there is no net consumption of O_2, as a molecule of O_2 is recovered from the reduction of the "spent"

catalyst with H_2O_2. This scenario does not obtain when other reductants are employed to regenerate the catalyst and drive the catalytic turnover.

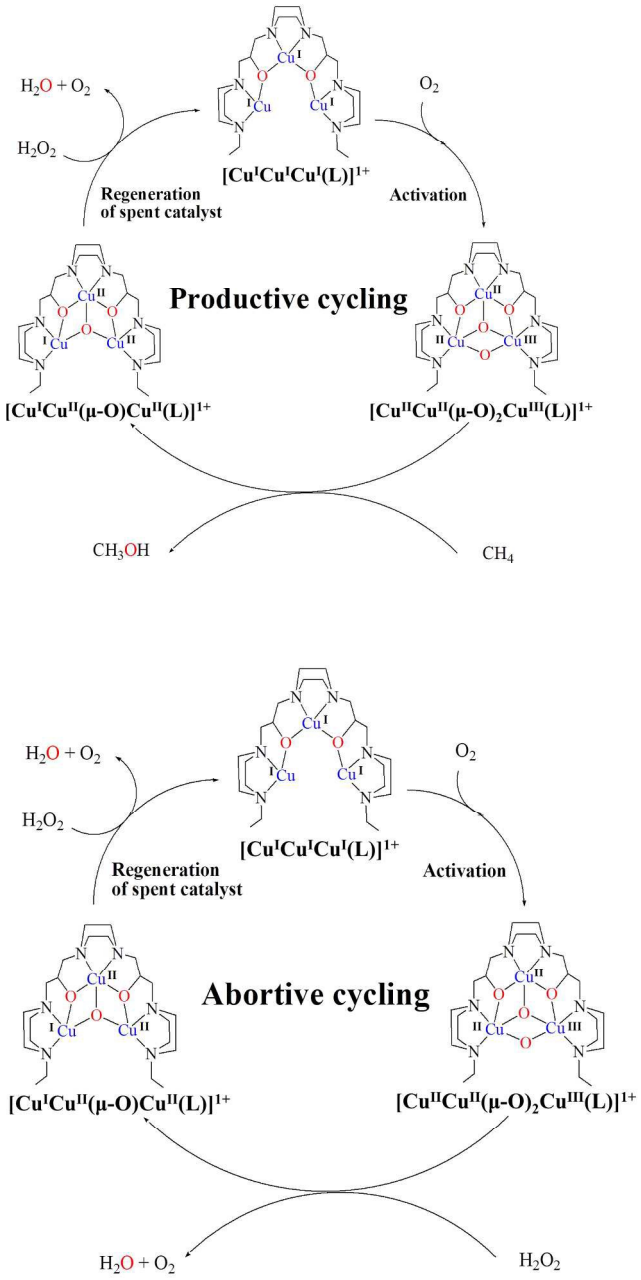

Scheme 2. ***Upper panel***: The turnover cycle driven by H_2O_2 in the catalytic oxidation of CH_4 mediated by the immobilized $[Cu^ICu^ICu^I(\mathbf{L})]^{1+}$ complex and O_2. ***Lower panel***: The abortive cycle of the catalytic system, a competing process that aborts the activated tricopper cluster by direct reduction with H_2O_2. **L** denotes the organic ligand **7-N-Etppz**

used to construct the tricopper cluster complex.

In Scheme 2, the turnover frequency (TOF) of the catalyst is determined by the rate of regeneration of the catalyst *via* reduction of the "spent" catalyst by H_2O_2. This is the rate-limiting step in the turnover cycle. The activation of the $[Cu^ICu^ICu^I(\mathbf{7\text{-}N\text{-}Etppz})]^{1+}$ catalyst by O_2 is extremely facile.[34] Without a CH_4 molecule occupying the hydrophobic substrate-binding cleft in the activated tricopper complex, however, the latter can be aborted by H_2O_2 as well. This abortive process (Scheme 2, *lower panel*) is also rapid because of the strong oxidizing power of the $[Cu^{II}Cu^{II}(\mu\text{-}O)_2Cu^{III}(\mathbf{7\text{-}N\text{-}Etppz})]^{1+}$ species.[30,31] When the tricopper complex is operated as a homogeneous catalyst in a solvent like MeCN, this abortive process limits the turnover number (TON) and the product yields due to the low solubility of CH_4 in the solvent. In fact, at sufficiently high concentrations of H_2O_2 used to drive the turnover, the productive cycling can be outcompeted by abortive cycling.[26,27] The outcome is that the tricopper complex is merely mediating the decomposition of the H_2O_2 used to drive the turnover to form O_2 and H_2O without the production of CH_3OH. Although the TOF is proportional to the concentration of H_2O_2 in the medium, it is evident that one must compromise between productive and aborting cycling to accomplish optimal performance of the catalyst for CH_3OH production.

Here, we describe the re-formulation of the tricopper cluster complex as a heterogeneous catalytic system for selective CH_4 oxidation by immobilizing the tricopper cluster complex into mesoporous silica nanoparticles (MSNs). The advantages of heterogeneous catalysis are numerous, including ease of product separation and recovery, recovery and reuse of the catalyst, as well as eventual scale-up of the process. The MSNs

are particularly suitable for immobilizing small compounds for chemical catalysis because of their surface areas, controllable geometric parameters, and a surface that can be conveniently modified to accommodate the types and sizes of molecules that can penetrate them.[35-38] With a particle size of ~80 nm, the MSNs can also be suspended in solution very well for the present application. Finally, but more significantly, this strategy of formulating the tricopper cluster catalyst allows us to exploit the over-solubility of CH_4 in the mesopores/nanopores of the functionalized MSNs to overcome some of the shortcomings of the homogeneous catalytic system described earlier.[26,27] It is now evident that the solubility of nonpolar gases like N_2, CH_4 and CO_2 can be as high as several hundred times higher than expected from the bulk solubility.[39-47] For these gases, the interactions of the gas molecules with the nanoporous solid or with the solvent are significantly weaker than the interactions of the solvent molecules with the walls of the confining host framework. The stronger solvent-solid interactions create regions of low solvent density in the confined solvent, enhancing gas uptakes.[47]. Thus, we expect that the mesopores/nanopores of the MSNs can accommodate large quantities of dissolved gases like CH_4 and O_2.

In this study, we have immobilized two tricopper complexes in MSNs and evaluated their performance toward selective conversion of CH_4 into CH_3OH. Indeed, we find that the heterogeneous catalyst can mediate the conversion of CH_4 into CH_3OH at room temperature with high catalytic efficiencies, high TONs, and excellent product yields, when the catalytic turnover is driven by H_2O_2.

Experimental section

Synthesis of the tricopper complexes

The synthesis and characterization of the ligands 3,3′-(1,4-diazepane-1,4-diyl)bis[1-(4-ethylpiperazine-1-yl)propan-2-ol] (**7-N-Etppz)** and 3,3'-(1,4-diazepane-1,4-diyl)bis[1-(4-ethylhomopiperazin-1-yl)propan-2-ol] (**7-N-Ethppz),** as well as the preparation of the $[Cu^{I}Cu^{I}Cu^{I}(\textbf{7-N-Etppz})]^{1+}$ and $[Cu^{I}Cu^{I}Cu^{I}(\textbf{7-N-Ethppz})]^{1+}$ complexes have been described earlier.[26,27,48] We have repeated the syntheses and preparations following these established procedures for the present study. Details are presented in Supplementary Information. (ESI,†) All solvents and chemicals used were of commercially available analytical grade, if not mentioned otherwise. Solvents for air-sensitive reactions were distilled under argon.

Synthesis of the negatively charged MSN-TP

In order to anchor the positively charged tricopper complexes to the surface of the MSN channels, we have functionalized the surface with the anionic 3-(trihydroxysilyl)propyl methylphosphonate (TP) to generate a negatively charged surface. The procedure is given as follow: 0.58 g of cetyltrimethylammonium bromide (C_{16}TAB) was dissolved in 300 g of 0.51 M ammonia solution ($NH_4OH_{(aq)}$) at 40 °C, and 5 ml of 0.21 M dilute tetraethyl orthosilicate (TEOS) solution (in ethanol (EtOH)) was added to the mixture. After stirring at 40 °C for 5 h, 250 µl of TP dissolved in 1 ml de-ionized H_2O and 5 ml of 0.88 M TEOS solution were added with vigorous stirring for another 1 h. The solution was then aged at 40 °C for 24 h. The as-synthesized materials were collected by centrifugation at 12,000 rpm for 25 min, washed and re-dispersed by EtOH several times. The surfactant templates were removed by extraction twice in ammonium nitrate/EtOH solution (1 g of ammonium nitrate/50 ml of EtOH at 60 °C for 1 h). Finally, the modified-MSN was collected by

centrifugation, washed with EtOH several times, and dried in vacuum for 10 h to obtain a colorless powder [$(MSN\text{-}TP)^{-}$ (NH_4^{+})].

Synthesis of the negatively charged AlMSN30-ex

0.386 g of $C_{16}TAB$ was dissolved in 160 g of 0.30 M $NH_4OH_{(aq)}$ at 50 °C. 1.2 ml of decane was dissolved in 15 ml of EtOH. Then, aqueous $C_{16}TAB$ solution was mixed with the decane/EtOH solution to form an oil-in-water emulsion by stirring. After the emulsion was stirred at 50 °C for 12 h, 1 ml of 0.167 M aluminum nitrate solution and 3.33 ml of 0.88 M TEOS/EtOH solution were mixed with vigorous stirring at 50 °C for 1 h. The solution was then aged at 50 °C for 24 h. Then the mixture containing the AlMSN30-ex and Al-MSF samples were separated by filter paper (55 mm). The filtrate containing the as-synthesized AlMSN30-ex sample was directly aged at 80 °C for 1 day to form the silica framework with high co-condensation. The as-synthesized material was then collected by centrifugation at 14,000 rpm for 30 min, washed and re-dispersed by EtOH several times. The surfactant templates were removed by extraction twice in ammonium nitrate/EtOH solution (1 g of ammonium nitrate/50 ml of EtOH at 60 °C for 1 h). Finally, the AlMSN30-ex sample was collected by centrifugation, washed with EtOH several times, and dried in vacuum for 10 h to obtain a colorless powder [$(AlMSN30\text{-}ex)^{-}$ (NH_4^{+})].

Immobilization of the $Cu^{II}Cu^{II}Cu^{II}$ tricopper complexes in the modified MSNs

10.0 mM of the exchange solution (solvent: 80% of MeCN and 20% of EtOH) containing the selected tricopper complex was prepared and used for the immobilization. First, 150 mg of the as-synthesized MSNs were well dispersed in 25 ml 99.5% EtOH, and then 25 ml of 10 mM exchange solution were added slowly and stirred at 30 °C for 24 h. The solids were collected by centrifugation, washed by 95% EtOH, and dried in vacuum.

The loadings of the tricopper complexes in the nanoparticles, henceforth referred to as **CuEtp**@MSN or **CuEthp**@MSN samples**,** were determined by measuring the copper content *via* ICP-MS experiments and the ligand content by C/N elemental analysis, and the results are given in **Table 2**.

Catalytic oxidation of CH_4 mediated by the CuEtp@MSN or CuEthp@MSN samples in the presence of H_2O_2

20 mg of **CuEtp**@MSN or **CuEthp**@MSN samples (including both the MSN-TP and AlMSN30-ex samples) were well suspended in anhydrous MeCN (5 ml) in a 50-ml glass sample bottle sealed tightly with a rubber cap. Then sodium ascorbate was added as a reducing agent (4 equivalent based on the amount of tricopper complex in the MSNs, freshly prepared 1 M solution in de-ionized H_2O) under a nitrogen atmosphere. The heterogeneous mixtures were stirred vigorously at room temperature to reduce the immobilized $Cu^{II}Cu^{II}(\mu\text{-}O)Cu^{II}$(**L**) complexes to their corresponding $Cu^{I}Cu^{I}Cu^{I}$(**L**) complexes (**L**, **7-N-Etppz** or **7-N-Ethppz**) *in situ*. The mixture was degassed, followed by injecting O_2 (10 ml at STP, 0.44 mmol) and CH_4 (100 ml STP, 4.4 mmol) using gas syringes to fill the total volume of the sample bottle with these two gases. After stirring for 10 min, an aliquot of either 100 equiv. or 200 equiv. of H_2O_2 solution (35%) was added. The reaction mixture was then stirred continuously for 3 h at room temperature. After breaking the seal to the glass sample bottle, 30 μl of nitrobenzene was added to the solution to provide an internal standard (IS) for quantitation of the products.

In the CH_4- or H_2O_2-limiting experiments, 60 mg of the **CuEtp**@AlMSN30-ex sample was well suspended in anhydrous MeCN (5 ml) in a 50-ml glass sample bottle sealed tightly with a rubber cap. For the CH_4-limiting experiments, 200 equiv. of H_2O_2 were used

to drive the catalytic turnover, and two different amounts of CH_4 were used: 15 ml and 30 ml of CH_4 at 1 atm, 30 °C, corresponding to 49.2 and 98.4 equiv., respectively. In the H_2O_2-limiting experiments, excess CH_4 (328 equiv., 100 ml of CH_4 at 1 atm, 30 °C) was used and the catalytic turnover was driven by 50 and 100 equiv. of H_2O_2. Otherwise, the reaction procedure was the same as in the normal CH_4 oxidation reaction described above.

The reaction solution was analyzed periodically by using GC-MS. The products of the CH_4 oxidation reaction were analyzed and confirmed by comparing with the commercially available standards (CH_3OH, MeCN, and nitrobenzene) and the built-in MS database software. Product yields and the turnover number are based on the loading of the tricopper complex in the MSNs.

Results

Immobilization of trinuclear copper complexes in mesoporous silica nanoparticles

Two kinds of silica nanoparticles have been employed for the present study (Scheme 3). In order to anchor the positively charged tricopper complex to the surface of the MSN nano-channels, we functionalize the surface with the anionic TP group to generate a negatively charged surface (MSN-TP). This conjugation of the silica by the negative TP group increases the loading of the tricopper complex. In addition, we prepare a pore-expanded MSN by adding decane[49] and increasing the surface charge density and acidity by doping Al into the framework (AlMSN30-ex).[50] Expansion of the silica pore and increasing the surface charge density can further increase loading of the immobilized complexes, which in turn can yield higher conversion of CH_4.

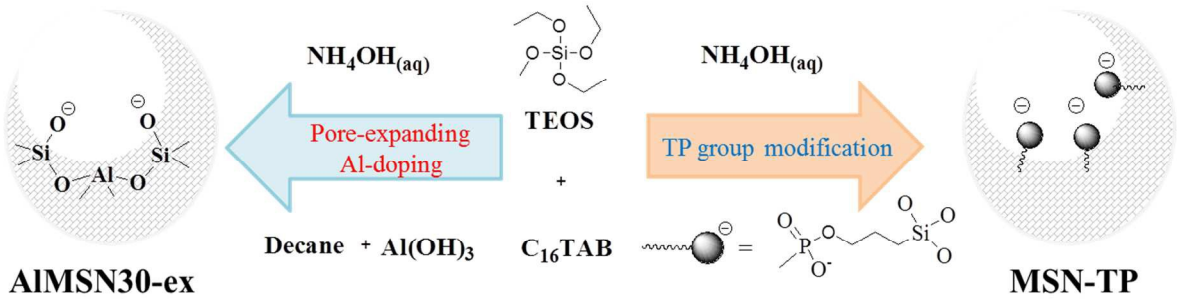

Scheme 3. Preparation of the two kinds of mesoporous silica nanoparticles (MSNs) used in this study. *Right*: In the MSN-TP sample, the surface of the MSNs is functionalized with the anionic TP to generate a negatively charged surface to anchor the positively charged tricopper complex to the surface of the nano-channels. *Left*: In the AlMSN30-ex sample, decane is used to expand the pore of the nano-channels and Al doping (Si/Al ratio = 30) is introduced into the framework to increase the surface charge density and acidity.

Two tricopper complexes have been selected for development of the heterogeneous catalyst for CH_4 oxidation using the two silica frameworks in this study: $[Cu^ICu^ICu^I$(**7-N-Etppz**)$]^{1+}$ and $[Cu^ICu^ICu^I$(**7-N-Ethppz**)$]^{1+}$. **7-N-Ethppz** differs from **7-N-Etppz** in the replacement of the six-membered piperazine ring in the latter by the seven-membered homopiperazine ring. The intent of this change in the ligand design is to tune the size and hydrophobicity of the hydrocarbon-binding cleft at the base of the assembled tricopper complex toward its recognition and binding of the hydrocarbon substrate.

We apply an ion-exchange method to immobilize the tricopper complexes in the functionalized MSN samples to obtain the following four formulations:

(1) **CuEtp**@MSN-TP: Cu_3(**7-N-Etppz**) complexes immobilized in the MSN-TP nanoparticles;

(2) **CuEthp**@MSN-TP: Cu_3(**7-N-Ethppz**) complexes immobilized in the MSN-TP nanoparticles;

(3) **CuEtp**@AlMSN30-ex: Cu_3(**7-N-Etppz**) immobilized in the pore-expanded MSNs with Al-doping (Si/Al ratio = 30); and

(4) **CuEthp**@AlMSN30-ex: Cu_3(**7-N-Ethppz**) immobilized in the pore-expanded MSNs with Al-doping (Si/Al ratio = 30).

Typically, the $Cu^{II}Cu^{II}(O)Cu^{II}(\mathbf{L})^{2+}$ form of the tricopper complex is immobilized in the functionalized MSNs and the $Cu^{I}Cu^{I}Cu^{I}(\mathbf{L})^{1+}$ catalyst is generated by reduction with ascorbate. The same results are obtained when the reduced tricopper complex is immobilized in the MSNs if the sample preparation is carried out in the glove box.

Physical characterization of the MSNs with the immobilized tricopper complexes

Transmission electron microscopy (TEM) images of the MSN samples (Fig. 1) demonstrate that the nanoparticles are well dispersed, with uniform sizes and clear evidence of nano-channels. The average particle diameter is about 80 nm. Statistical analysis (Fig. 1, *inset*) of the TEM images gives a particle size distribution of 71.4 ± 7.8 nm for the MSN-TP sample (based on a patch size of 100 particles) and 67.7 ± 6.0 nm for the AlMSN30-ex preparation (based on a patch size of 70 particles). The expanded-pore AlMSN30-ex sample has a pore diameter of 4.8 ± 0.57 nm, and shows cleaner mesopores than the MSN-TP sample, which has a pore diameter of 2.8 ± 0.14 nm (Fig. S1). Doping aluminum into the framework of the MSN-ex sample does not appear to affect the size of the nano-silica particles or the definition of nano-channels. ^{29}Si solid-state NMR of the AlMSN30-ex and the MSN-TP samples (Fig. 2) indicate that the MSN samples are formed with a high degree of silica poly-condensation with mainly Q3 and Q4 substructure.[49,50] Al solid-state NMR of the AlMSN30-ex sample (Fig. 2d) reveals only

Al^{3+} occupying the tetrahedron site of Al in the silica framework, indicating good co-condensation.

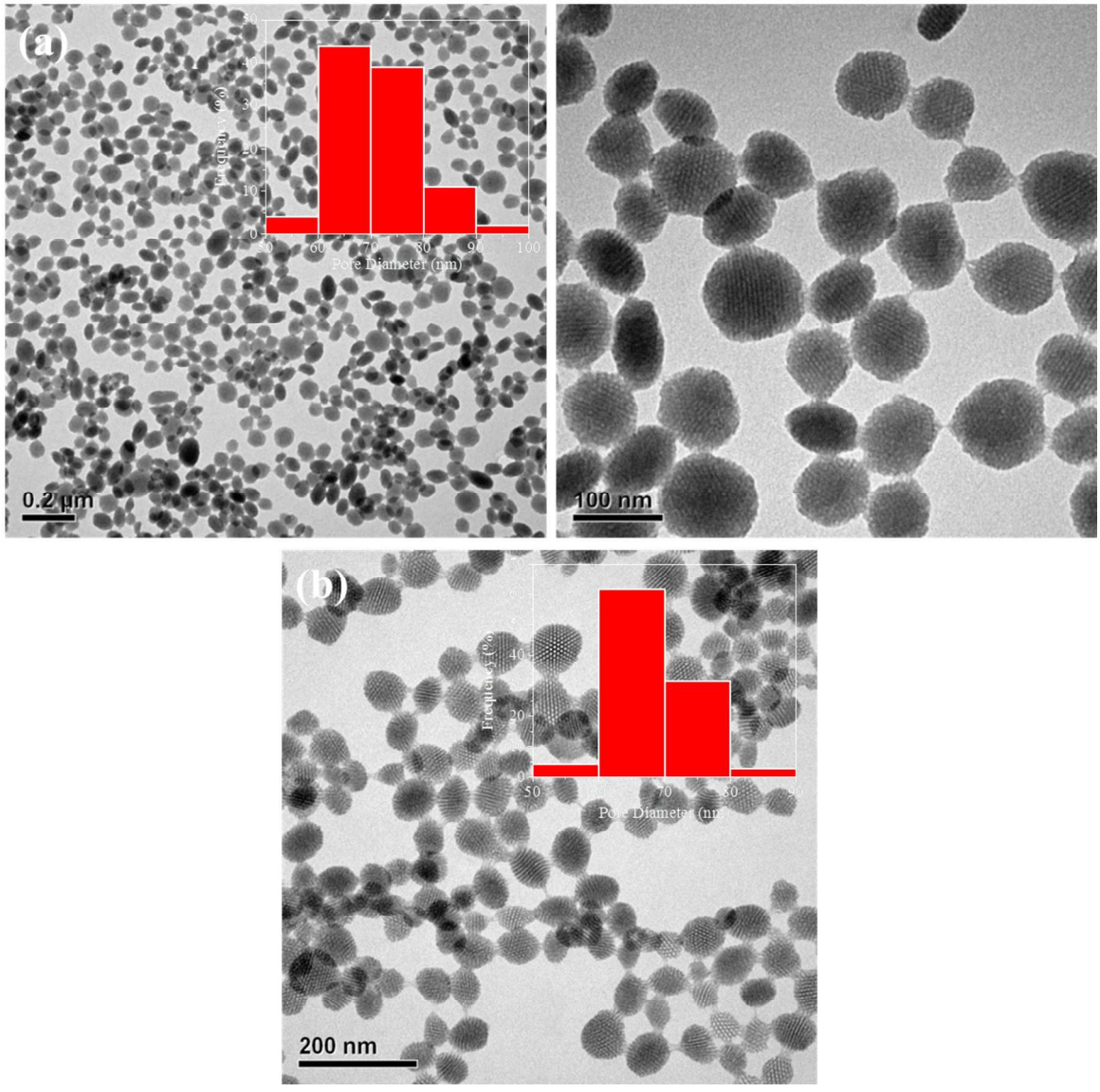

Fig. 1. Transmission electron microscopy (TEM) images of the functionalized MSN samples: (**a**) MSN-TP sample with different scale bars (*left*: 0.2 μm; *right*: 100 nm); and (**b**) AlMSN30-ex sample with 200 nm scale bars. Statistical analysis of the TEM images gives a particle size distribution of 71.4 ± 7.8 nm for the MSN-TP sample (Fig. 1a *left,*

inset, based on a patch size of 100 particles) and 67.7 ± 6.0 nm for the AlMSN30-ex preparation (Fig. 1b, *inset*, based on a patch size of 70 particles).

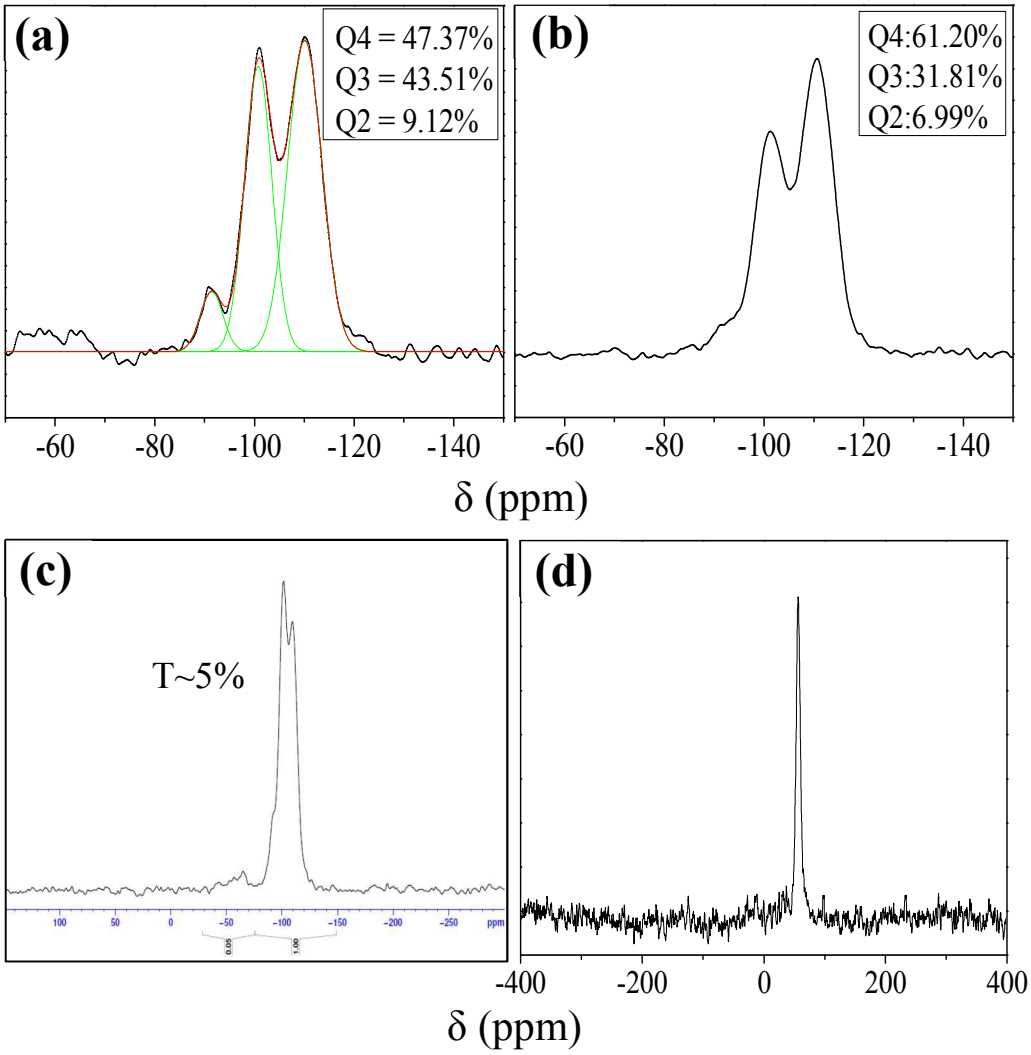

Fig. 2. ^{29}Si solid-state NMR spectra of the functionalized MSN samples: (**a**) MSN-TP; and (**b**) AlMSN30-ex. Each spectrum displays a set of signals Q2, Q3, and Q4, attributed to the $Si(OH)_2(OSi)_2$, $Si(OH)(OSi)_3$, and $Si(OSi)_4$ substructures, respectively. The peak percentages are obtained by de-convoluting each spectrum into their components and fitting the full-width at half-maximum of each component spectrum. (**c**) ^{29}Si NMR spectrum of the MSN-TP sample, comparing the T signals ([C-$Si(OH)(OSi)_2$] or [C-

$Si(OSi)_3$]) to the Q signals. Ratio of the areas of the T and Q signals indicates that 5% of the silica surface is conjugated to the functionalizing TP group. (**d**) ^{27}Al solid-state NMR spectrum of the AlMSN30-ex sample. The chemical shift indicates that the Al is co-condensed with the TEOS in the framework (~56 ppm).

Table 1. Physical properties of the MSN samples with the immobilized tricopper complexes Cu_3(**7-N-Etppz**) and Cu_3(**7-N-Ethppz**).

Sample Name	Surface Area (m^2/g)	Pore Volume (cm^3/g)	Pore Diameter (nm)	Complex Adsorption (μmol/g)	Zeta-potential (ζ) (mv)	
					ζ (mv)	[a]Δζ (mv)
MSN-TP	912.4	0.71	2.8	-	−36.2	-
CuEtp@MSN-TP	701.9	0.39	1.7	114	−22.6	+13.6
CuEthp@MSN-TP	742.2	0.41	1.8	103	−24.0	+12.2
AlMSN30-ex	1242.1	1.43	4.8	-	−46.1	-
CuEtp@AlMSN30-ex	758.9	0.90	2.6	204	−14.9	+31.2
CuEthp@AlMSN30-ex	803.9	0.93	2.8	184	−18.3	+27.8

[a]Δζ: The change of the values of the zeta-potential after immobilization of the tricopper complexes in the MSNs.

Loading of the tricopper complex

In the preparation of the tricopper-complex loaded MSNs, the concentration of the tricopper complex solution used in the immobilization is 10 mM. This concentration is selected, as it is the lowest concentration of the tricopper complex to give close to saturation of the monolayer adsorption. For the negatively charged MSN-TP samples, the amount of loading of the Cu_3(**7-N-Etppz**) (114 μmol of complex / 1 g of sample) is somewhat higher than that of the Cu_3(**7-N-Ethppz**) (103 μmol of complex / 1 g of sample). However**,** when the silica pore size is expanded to 4.8 ± 0.57 nm and the surface charge density increased by Al-doping of the framework, the loading of the tricopper complex

increases about one fold (**CuEtp**@AlMSN30-ex: 204 μmol/g, and **CuEthp**@AlMSN30-ex: 184 μmol/g) relative to those of the corresponding MSN-TP samples (pore size: 2.8 ± 0.14 nm). These results are supported by Zeta-potential measurements and BET analysis, as shown in Table 1**.**

The amounts of the tricopper complexes immobilized in the various MSN samples are determined from the copper contents obtained by ICP-Mass analysis and the ligand contents by C/N elemental analysis. As shown in Table 2, the copper-to-ligand molar ratios of the four MSN samples loaded with the tricopper complexes are very close to the stoichiometric values of the tricopper complexes. That the tricopper complexes remain intact during the immobilization in the functionalized MSN samples is confirmed by electron paramagnetic resonance (EPR) measurements on the MSN samples (Fig. S2, ESI,†), which, in each case, exhibits an EPR signal expected of a spin-frustrated $Cu^{II}Cu^{II}Cu^{II}$ spin system at liquid nitrogen temperature.[51] The observed differences in the Cu^{2+} EPR spectra between the **CuEtp**@MSN-TP and **CuEtp**@AlMSN30-ex samples may be attributed to the greater site heterogeneity of the tricopper complexes within the nano-channels of the **CuEtp**@AlMSN30-ex system. EPR provides a sensitive probe of the structural heterogeneity of the fully oxidized tricopper complex located in different regions of the nano-channels. With a capping "oxo", the EPR spin-Hamiltonian parameters associated with the three unpaired electrons of the Cu^{II} triad of the oxidized $[\{Cu^{II}Cu^{II}(\mu\text{-}O)Cu^{II}\}(\mathbf{L})]^{2+}$ complex, especially the electrostatic super-exchange interactions between adjacent spins, are sensitive to the dome-ness of the bridging "O^{2-}", The dome-ness of the capping "oxo" is in turn influenced by its interactions with the environment of the tricopper complex in the MSNs. Accordingly, the structural

heterogeneity reflects the site heterogeneity, which is expected to be present in the undulating pores of the MSN sample. In any case, the EPR data provide us with an important spectroscopic control to ensure that the $[\{Cu^{II}Cu^{II}(\mu\text{-}O)Cu^{II}\}(\mathbf{L})]^{2+}$ complex has been assembled correctly before reduction by ascorbate to form the fully reduced $[\{Cu^{I}Cu^{I}Cu^{I}\}(\mathbf{L})]^{1+}$ complex, which is EPR silent. It is the $[\{Cu^{I}Cu^{I}Cu^{I}\}(\mathbf{L})]^{1+}$ tricopper cluster complex that is the functional catalyst.

Table 2. Compositions of the Cu_3(**7-N-Etppz**)- and Cu_3(**7-N-Ethppz**)-immobilized MSN samples: Contents and mole ratios.

Sample	[a] µmol of Cu per gram of sample	[b] µmol of ligand per gram of sample	Cu / ligand ratio
CuEtp@MSN-TP	345.2	113.8	3.03
CuEthp@MSN-TP	310.1	102.6	3.02
CuEtp@AlMSN30-ex	612.9	203.6	3.01
CuEthp@AlMSN30-ex	556.3	183.6	3.03

[a] Copper content is determined by ICP-Mass experiments.
[b] Ligand content is based on results from C/N elemental analysis.

In leaching tests, we observe loss of no more than 25 ppm (~0.0025%) of the tricopper complexes from each of the MSN samples after stirring for 10 h at 25 °C. (Table S1, ESI,†). Note that these leaching experiments are carried out on the $Cu^{II}Cu^{II}Cu^{II}$ complexes immobilized in the MSNs, not under conditions in which the tricopper catalyst is turning over (*vide infra*).

Catalytic conversion of CH_4 into CH_3OH by H_2O_2 mediated by the tricopper-complexes in the presence of O_2 in the MSNs

As expected, the tricopper complexes immobilized in the various MSN samples support the catalytic conversion of CH_4 into CH_3OH after reduction of the $Cu^{II}Cu^{II}Cu^{II}$ complexes by a stoichiometric amount of ascorbate to form the $Cu^{I}Cu^{I}Cu^{I}$ complexes. This reduction of the tricopper complexes is performed by adding a slight excess (*ca*. 4 equiv.) of sodium ascorbate in 250 μl H_2O into a flask containing 20 mg sample of the MSNs in 5 ml of MeCN. After stirring for 10 min and vacuum drying, 100 ml of CH_4 (986-1953 equiv., based on the catalyst) and then 10 ml of O_2 (98.6-195.3 equiv., based on the catalyst), each at a pressure of 2.44 atm, are injected into the sample. An aliquot of either 100 equiv. or 200 equiv. of H_2O_2 solution (35%) is then added, and the reaction mixture is stirred continuously for 3 h at room temperature. At various intervals over this 3-h period, an aliquot of the solution is withdrawn for GC-MS analysis to monitor the formation of CH_3OH (and other possible products).

Turnover numbers. Fig. 3 summarizes the TONs observed at various times for each of the four MSNs studied when the turnover of the catalyst is initiated with 200 equiv. of H_2O_2. These heterogeneous formulations of the tricopper complexes can be seen to be highly active toward CH_4 oxidation. As expected, dramatically higher TONs are obtained when the $[Cu^{I}Cu^{I}Cu^{I}(\textbf{7-N-Etppz})]^{1+}$ tricopper complex is reformulated as a heterogeneous catalyst compared to when it was used earlier as a homogeneous catalyst for CH_4 oxidation in MeCN.[26,27] This comparison is depicted for the **CuEtp**@AlMSN30-ex formulation in Table 3. As a homogeneous catalyst, only a maximum TON of 6.5 was observed when the catalytic turnover was initiated by 20 equiv. of H_2O_2, and essentially no CH_3OH was detected with 200 equiv. of H_2O_2.[27] Interestingly, reasonable TONs are now obtained for the **CuEthp**@MSN-TP formulation. In our earlier study on CH_4

oxidation by homogeneous formulations of the tricopper cluster complexes, no CH_4 oxidation was observed with the Cu_3(**7-N-Ethppz**) complex.[30] Even for the present heterogeneous MSN formulations, however, the TONs are dramatically lower for the Cu_3(**7-N-Ethppz**) catalyst, underscoring the importance of substrate recognition of the catalyst to control futile cycles (*vide infra*). By comparison, the effects of Al-doping seem relatively minor, when we compare the TONs between the **CuEtp**@MSN-TP and the **CuEtp**@AlMSN30-ex samples, and between the **CuEthp**@MSN-TP and the **CuEthp**@AlMSN30-ex formulations. As expected, the CH_4 conversion yields are about double for the formulations with the Al doping because of approximately twice the loading of the MSN samples. Since the amounts of CH_4 (O_2 as well) are in significant excess within the system in each of these experiments, the CH_4 conversion yield depends on the amounts of the starting CH_4. Accordingly, it is only meaningful to compare CH_4 conversion yields when the experiments are conducted using the same amounts of CH_4.

According to the TON criterion, the **CuEtp**@AlMSN30-ex formulation is the best performing catalyst. To delineate the operational characteristics of this heterogeneous formulation, we have compared the turnover when it is driven by 50, 100 and 200 equiv. of H_2O_2 (Fig. S3, ESI,†). The TON increases more or less proportionally with the amount of starting H_2O_2 used. From the limiting TONs obtained in each case, we have concluded that the tricopper complex in the MSNs is activated by O_2, not H_2O_2, just as we had hoped for. When the tricopper complex is activated by H_2O_2, two additional H_2O_2 molecules are consumed per catalytic cycle, and the limiting TONs would be lower by a factor of 3 based on the amount of H_2O_2 available for the turnover.[52] In contrast, there is no overall consumption of O_2 when tricopper catalyst is activated by O_2. As noted earlier, a molecule

of O_2 is produced in the regeneration of the catalyst in the turnover cycle, replacing the molecule of O_2 that is consumed in the initial activation step.

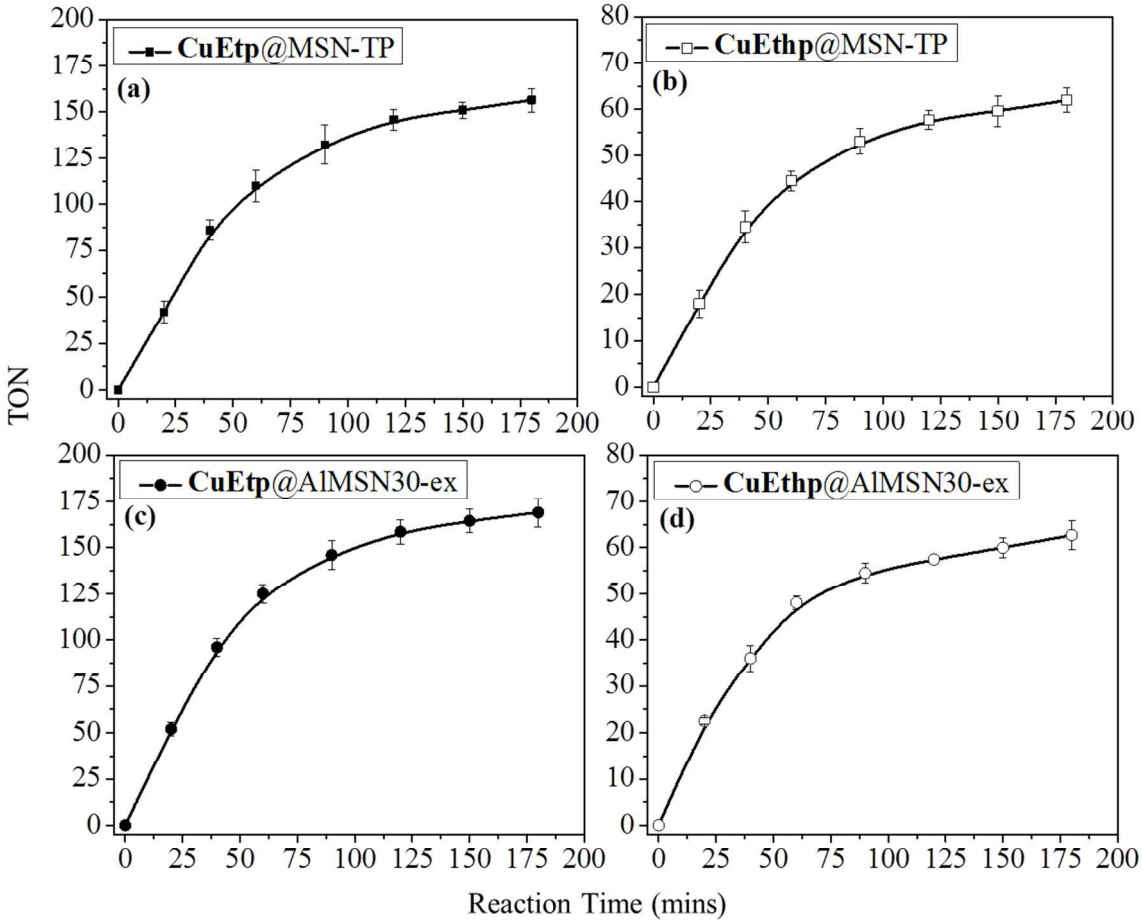

Fig. 3. The time course of the TONs for the CH_4 oxidation reaction catalyzed by each of the two tricopper complexes immobilized into the two types of MSNs at room temperature. The catalytic turnover is initiated with 200 equiv. of H_2O_2: (**a**) **CuEtp**@MSN-TP; (**b**) **CuEthp**@MSN-TP; (**c**) **CuEtp**@AlMSN30-ex; and (**d**) **CuEthp**@AlMSN30-ex. In each case, the MSN sample is well dispersed in O_2-free MeCN before 100 ml of CH_4 and 10 ml of O_2, each at a pressure of 2.44 atm, are injected into the sample. After stirring for 10 min, an aliquot of 200 equiv. of H_2O_2 solution (35%) is finally added. The TONs of CH_3OH are expressed by moles of CH_3OH formed per mole of the tricopper complex mediating the catalytic conversion of CH_4 into CH_3OH.

Table 3. Comparison of the performance (limiting TONs) of **Cu_3(7-N-Etppz)** complex as a homogeneous catalyst for conversion of CH_4 into CH_3OH *versus* its reformulation as a heterogeneous catalyst in AlMSN30-ex nanoparticles at room temperature.

Cu_3(**7-N-Etppz**)			**CuEtp@AlMSN30-ex**		
Homogeneous			**Heterogeneous**		
H_2O_2 (equiv.)	TON_{CH3OH}	[a]OCE	H_2O_2 (equiv.)	TON_{CH3OH}	[a]OCE
0	1	-	0	1.0	-
20	6.5	0.33	20	15.9	0.80
40	~0	~0	50	42.5	0.85
100	~0	~0	100	81.1	0.81
180	~0	~0	200	171.2	0.86

[a] OCE denotes the overall catalytic efficiency, as estimated by the ratio of the CH_3OH produced (N_{CH3OH}) in the experiment to the amount of H_2O_2 used to initiate the turnover (N_o), namely, N_{CH3OH}/N_o (see text).

Catalytic efficiencies. In addition, the overall catalytic efficiency (OCE) of the **CuEtp**@AlMSN30-ex sample is very high (see Tables 3 and 4). The OCE denotes the effectiveness of the $[Cu^ICu^ICu^I(\mathbf{L})]^{1+}$ complex as a catalyst for CH_4 oxidation based on the starting amount of H_2O_2 used to drive the turnover. It is given by the ratio of the yield of CH_3OH at the end of the catalytic run (N_{CH3OH}) to the amounts of H_2O_2 used to initiate the catalysis (N_o). According to the stoichiometry depicted in Scheme 2, OCE = $N_{CH3OH}/N_o \leq 1$. It is 100% if every H_2O_2 molecule is consumed and contributes to the production of a CH_3OH molecule.

Table 4 summarizes the TONs, product yields, and OCEs for the four formulations, when the turnovers are initiated with 100 and 200 equiv. of H_2O_2 (starting with the same amounts of CH_4). With **CuEtp**@AlMSN30-ex, our best performing catalyst, we obtain a limiting TON number of 171 using 200 equiv. of H_2O_2 and 81 using 100 equiv. of H_2O_2. These results are remarkable as the OCEs are greater than 80%, with the bulk of the H_2O_2 consumed in turning over the tricopper catalyst for CH_4 oxidation. Given that as not all the

H_2O_2 added to initiate the CH_4 oxidation is actually available for turnover of the catalyst, abortive cycling of the tricopper catalyst must be very low. At sufficiently low H_2O_2 concentrations, this reductant no longer has sufficient reducing power to regenerate the catalyst, especially with the amounts of O_2 present in the medium. In a typical turnover experiment, the catalysis eventually stops, yielding the limiting TON with some amounts of the initial H_2O_2 remaining in the solution.

Table 4. The limiting TONs, conversions, and OECs of CH_4 oxidation mediated by the Cu_3(**7-N-Etppz**) and Cu_3(**7-N-Ethppz**) tricopper complexes immobilized in the two MSN formulations.[a]

Sample Name	100 equiv. $H_2O_{2(aq)}$			200 equiv. $H_2O_{2(aq)}$		
	[b]TON	[c]Conversion	[d]OCE	[b]TON	[c]Conversion	[d]OCE
CuEtp@AlMSN30-ex	81.1	8.23	0.81	171.2	17.4	0.86
CuEthp@AlMSN30-ex	24.4	2.23	0.24	63.3	5.79	0.32
CuEtp@MSN-TP	78.4	4.44	0.78	156.5	8.87	0.78
CuEthp@MSN-TP	19.6	1.00	0.20	60.5	3.10	0.30

[a]These data represent the average of three separate experiments using the same formulation of a given catalyst.
[b] TON = moles of CH_3OH produced per mole of tricopper complex immobilized in the MSNs.
[c] Conversion = moles of CH_3OH produced per mole of CH_4 injected) × 100%.
[d] OCE denotes the overall catalytic efficiency measured by the ratio of the CH_3OH produced (N_{CH_3OH}) in the experiment to the amount of H_2O_2 used to initiate the turnover (N_o).

The OEC provides an overall index of performance of our catalytic system, A better measure of the performance of the tricopper catalyst is offered by the catalytic efficiency (CE) defined by the ratio of the number of productive turnovers of the catalyst to the total

number of turnovers including both productive and abortive cycles during the course of the experiment.[27] As the CE is directed at the operations of the tricopper complex itself, it measures the efficacy of the complex to convert CH_4 into CH_3OH at the molecular level. For example, upon activation of the tricopper catalyst by O_2, productive cycling of the catalyst gives one CH_3OH product per H_2O_2 consumed. However, a futile cycle takes place when the activated tricopper catalyst is reduced (and aborted) by a molecule of H_2O_2 to produce O_2 and H_2O instead of reacting with CH_4 to form CH_3OH. Thus, the CE is given by

$$n_{productive}/(n_{prodcutive} + ½ \times n_{abortive}) = N_{CH3OH}/(N_o - ½ \times n_{abortive} - n_{remaining}),$$

where N_o, $n_{prodcuctive}$, $n_{abortive}$, and $n_{remaining}$ denote the amount of H_2O_2 used to initiate the catalysis (defined earlier), the amount consumed by productive cycling, the amount consumed by abortive cycling, and H_2O_2 remaining in the solution at the end of the catalytic run, respectively. Comparing the CE and OCE, it follows that CE ≥ OCE; moreover, if N_{CH3OH}/N_o or the OCE exceeds 80%, CE must approach 100%. If so, $n_{abortive}$ and $n_{remaining}$ must be low.

For our most efficient heterogeneous formulation of the catalyst, namely, CuEtp@AlMSN30-ex, OCE = 81% and 86% for $[H_2O_2\}_0$ = 100 equiv. and 200 equiv., respectively. According to the above expressions for CE and OEC, the OEC should decrease at the higher $[H_2O_2]_0$ used to initiate the catalytic turnover. The reverse trend is observed. In the case of CuEtp@MSN-TP, OCE = 78% for both $[H_2O_2\}_0$ = 100 equiv. and 200 equiv. Thus, it is evident that abortive cycling is not significant in the turnover for our catalytic formulations. Rather, the data indicate that not all the H_2O_2 used to initiate the

catalysis are consumed for turnovers, productive or abortive. The data are consistent with about 10% of the H_2O_2 remaining in the system.

Clearly, with an OCE in excess of 80% when the catalysis is initiated with 100 or 200 equiv. of H_2O_2, the **CuEtp**@AlMSN30-ex is functioning extremely well as a CH_4 oxidation catalyst. The performance of the **CuEtp**@MSN-TP catalyst is similar, with an OCE approaching 80% when it is operated under the same conditions. In contrast, the **CuEthp**@AlMSN30-ex and **CuEthp**@MSN-TP catalysts perform relatively poorly, with OECs of only ~30% and ~20% when these catalysts are turned over with 200 equiv. and 100 equiv. of H_2O_2, respectively. Clearly, abortive cycling must be accompanying productive cycling with these two catalysts. We will compare the performance of the **CuEtp**@MSN and **CuEthp**@MSN catalysts more fully later.

Product yields. It is customary to assess the overall performance of a catalyst by comparing product yields. Although the conversion yields for the aforementioned experiments are only 17.4% and 8.23%, respectively (Table 4), these numbers do not provide a good measure of performance of the catalytic system, as noted earlier. The CH_4 concentration is significantly higher than the H_2O_2 concentration used to perform the turnover so that the H_2O_2 is depleted or its reducing power spent well before the CH_4 available to the catalyst is exhausted. In any case, the amounts of CH_3OH produced are substantial in the two experiments. When the turnover is mediated by the **CuEtp**@AlMSN30-ex formulation using 200 equiv. of H_2O_2, the concentration of CH_3OH in the final solution is *ca*. 133 mM.

To illustrate this point further, we have undertaken CH_4-limiting experiments, in which the amount of CH_4 available for oxidation is less than the amount of H_2O_2 added to drive

the turnover. The outcome of this experiment is shown in Fig. 4a. Here, 200 equiv. of H_2O_2 are used to drive the catalytic turnover, and two different amounts of CH_4 are used: 15 ml and 30 ml of CH_4 at 1 atm, 30 °C, corresponding to 49.2 and 98.4 equiv., respectively. In the experiment corresponding to the lower amount of CH_4, the limiting TON obtained is 48.1, and for the higher amount of CH_4, 97.8. These TONs correspond essentially to 100% conversion of the CH_4 into CH_3OH; in other words, total consumption of the CH_4 available to the catalyst, or the maximum numbers of turnovers possible commensurate with the amount of CH_4 available for oxidation.

For comparison, we have also undertaken the above CH_4 oxidation experiments using excess CH_4 (328 equiv., 100 ml of CH_4 at 1 atm, 30 °C), but under H_2O_2-limiting conditions (50 and 100 equiv.). The results are shown in Fig. 4b. As expected, the limiting TONs are not as high as might be expected on the basis of the amounts of H_2O_2 added to initiate the turnover. At 50 and 100 equiv. of H_2O_2, abortive cycling is not an issue. However, as noted earlier, at sufficiently low concentrations, H_2O_2 is no longer a good reductant to regenerate the catalyst under the conditions of these experiments. In any case, despite the rather comparable TONs observed, the product yields are substantially lower, as a percentage of the CH_4 converted.

Regardless of the TONs, catalytic efficiencies or product yields, the tricopper catalyst is robust, and the catalytic activity can be sustained further (up to 6 h) by simply injecting additional H_2O_2 (50 equiv., 100 equiv., or 200 equiv.) into the suspension of MSNs (Fig. S4, ESI,†). In contrast, the injection of only additional CH_4 into the system does not enhance the TONs as the CH_4 gas is already in excess, a manifestation of the over-solubility of CH_4 in the MeCN confined in these mesoporous silica nanoparticles.

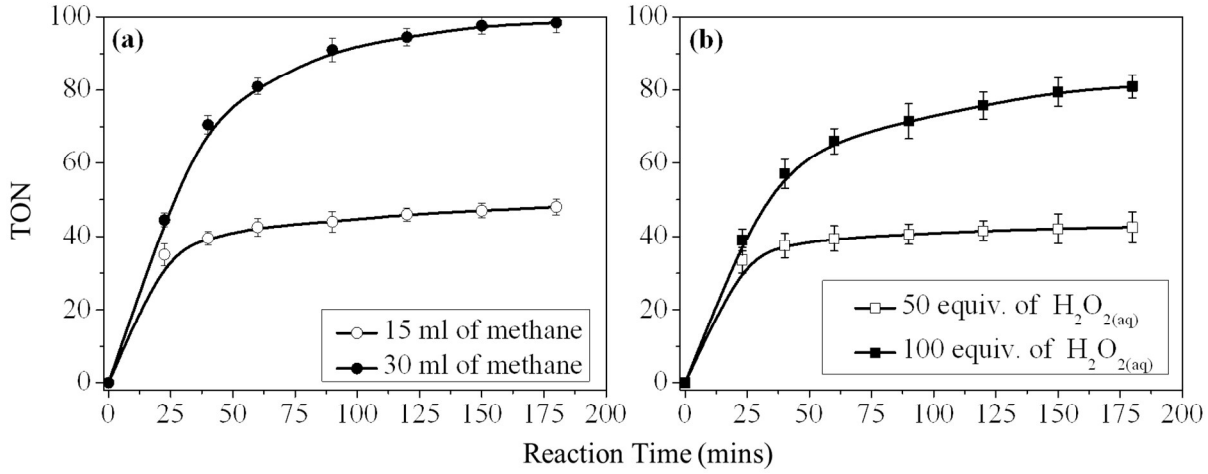

Fig. 4. The time course of TONs for the CH_4 oxidation reaction catalyzed by the **CuEtp**@AlMSN30-ex formulation at room temperature with (**a**) limiting CH_4 (1 atm, 15 ml (○); and 1 atm, 30 ml (●)) and (**b**) limiting H_2O_2 (50 equiv. (□); and 100 equiv. (■)) for 3 h.

Turnover frequencies. From the limiting slopes of the TONs *versus* time plots in Fig. 3, we can estimate the turning over frequencies (TOFs) of the catalyst for the two heterogeneous formulations of the two tricopper complexes. For **CuEtp**@AlMSN30-ex, our best formulation, the TOF at the beginning of the experiment after adding 200 equiv. of H_2O_2 to the suspension is ~2.11 min^{-1} or about 3.5×10^{-2} s^{-1} (or 127 h^{-1}). Note that this quantity should be directly proportional to the concentration of H_2O_2 available in the medium to drive the turnover, so the TOF decreases as the turnover progresses. In any case, the highest rate at which we have been able to turn the catalyst over is *ca.* 10% of k_{cat} estimated for the pMMO in *M. capsulatus* (Bath).[30,31] However, the two catalytic systems are not directly comparable. In the case of our tricopper-complex formulation, the TOF is controlled by the rate of reduction of the "spent" catalyst to regenerate the catalyst. The

rate of O-atom transfer from the activated catalyst to the CH_4 is many orders of magnitude more facile. In the enzyme, the factors controlling k_{cat} are much more complex. Similarly, the TOF of our best performing catalyst is an order of magnitude lower than that reported for the Cu-Fe-ZSM-5 catalytic system by Hutchings *et al*.[17,18] This group uses H_2O_2 as the terminal oxidant to activate di-oxo di-iron clusters in the zeolite to convert CH_4 to CH_3OOH, which is then subsequently reduced by a Cu^{II}-mediated process to form CH_3OH. Accordingly, it is difficult to accomplish with the Cu-Fe-ZSM-5 system the same degree of product selectivity that is possible with our tricopper-complex catalyst. Our catalyst is totally selective to yield CH_3OH. Moreover, because of the significantly higher loading of the **CuEtp**@AlMSN30-ex catalyst, the amounts of CH_3OH produced per weight of catalyst are actually higher by more than 10-fold, with a significantly lower consumption of H_2O_2. In any case, with our biomimetic catalyst, it is possible, in principle, to develop more efficient reductants or methods to enhance the TOF.

Further comparison of the CuEtp@MSN and CuEthp@MSN catalysts. The differences between the Cu_3(**7-N-Etppz**) and Cu_3(**7-N-Ethppz**) tricopper complexes in their catalytic efficiencies for CH_4 conversion into CH_3OH in the MSNs are dramatic. Structurally, the Cu_3(**7-N-Ethppz**) tricopper complex exhibits a bigger hydrophobic cleft at the base of the copper triad compared with the Cu_3(**7-N-Etppz**) complex. Recognition of the CH_4 substrate is critical to the formation of the hydrocarbon-catalyst complex that culminates in the transition state for ultimate O-atom transfer to generate the product CH_3OH. For this purpose, the smaller cleft constructed at the base of the Cu_3(**7-N-Etppz**) complex is more suitable for effective binding of a small symmetric substrate such as CH_4. CH_4 recognizes and binds to the hydrophobic pocket of the Cu_3(**7-Ethppz**) complex as

well, but the binding is less restricted resulting in greater conformational entropy of the CH_4 molecule in the larger hydrophobic pocket. In contrast, the reaction of the activated tricopper complex with H_2O_2 probably occurs *via* formation of an inner-sphere complex with the exposed "O" atom of the $Cu^{II}Cu^{II}(\mu\text{-}O)_2Cu^{III}$ species in the abortive process (see Scheme 2). If so, the abortion of the activated tricopper cluster should be relatively insensitive to this structural difference in the hydrocarbon recognition and binding cleft. Given that we observe no abortive cycling in the case of the **CuEtp**@MSN catalyst, we surmise that $k_{OT} >> k_{AB,}$ for the turnover mediated by the Cu_3(**7-N-Etppz**) complex, where k_{OT} and k_{AB} denote the second-order rate constants for the O-atom transfer to the C−H bond in CH_4 during the productive cycling and the abortive reduction by H_2O_2 in the abortive cycling described by the upper and lower *panels* in Scheme 2, respectively. Since the onset of abortive cycling would begin to manifest itself when $k_{OT}\,[CH_4] \approx k_{AB}\,[H_2O_2]$, we conclude that $k_{OT} \leq k_{AB}$, in the case of the Cu_3(**7-N-Ethppz**) complex.

Heterogeneous catalysis? Up to this point, we have assumed that the conversion of CH_4 into CH_3OH mediated by tricopper complexes in the MSNs to be a quasi-heterogeneous process. In other words, the conversion is mediated by the tricopper complex immobilized in the MSNs with the catalyst activated by O_2 in the mesopores/nanopores of the nanoparticles and transferring one of the O atoms to a CH_4 molecule solubilized in the MSNs, and the H_2O_2 needed to complete the catalytic turnover taken from the bulk solution phase in which the MSNs are suspended. To verify this assumption, we have tested for catalytic activity of the bare MSNs, including both the MSN-TP and AlMSN30-ex samples (Fig. S5, ESI,†). We have also examined the solution phase of the **CuEtp**@AlMSN30-ex formulation (and also the **CuEthp**@AlMSN30-ex

formulation) for further CH_4 oxidation, after removing the nanoparticles from the solution by centrifugation following a 40-min catalytic turnover, until the end of the 3-h experiment (Fig. S6, ESI,†). No catalytic activity is detected with the bare MSNs or for the solutions without the nanoparticles. Thus, the catalytic activity is intrinsic to the active tricopper complex immobilized in MSNs, and the catalysis is heterogeneous.

Finally, to ensure that the immobilized tricopper catalyst is not triggering auto-oxidation to promote the CH_4 oxidation, we have also performed a parallel control experiment in which the CH_4 oxidation is mediated by the **CuEtp**@AlMSN30-ex formulation (as well as the **CuEthp**@AlMSN30-ex formulation) at room temperature in the presence of the radical trapping agent 2,6-di-*tert*-butyl-*p*-cresol.[50] We have detected no apparent effect of the radical trapping agent on the TONs or product yields throughout the time course of the experiment (Fig. S7, ESI,†). Thus, we conclude that the CH_4 oxidation observed with our heterogeneous formulations is not promoted by auto-oxidation triggered by the immobilized tricopper complex.

Reuseability of the MSNs

The MSN formulations of the tricopper complexes are reuseable. To verify this, we have examined the TONs of the CH_3OH obtained from the CH_4 oxidation reaction catalyzed by **CuEtp@**AlMSN30-ex sample at room temperature with 200 equiv. of H_2O_2 for three cycles at varying times. The samples are easily separated from the reaction mixture and dried by vacuum after each reaction cycle before performing the next. Evidently, there is a loss in the activity of the catalyst after each 3-h run (Fig. 5). The drop off in activity corresponds to ~10% per cycle. After each cycle, the Cu content of the collected **CuEtp**@AlMSN30-ex was determined by ICP-MS and the ligand content by

C/N elemental analysis before performing the next. It is apparent from these data that the decrease of activity arises from ~10% loss of the tricopper complex during the catalytic run, due to either dissociation of the complex from the nanoparticles or decomposition of the tricopper complex. If the data in Fig. 5a, are corrected for the suggested loss of the tricopper complex, the TONs based on the remaining tricopper-complex content are superimposable on one another (Fig. 5b). With accumulation of CH_3OH and H_2O in the medium supporting the MSNs following sustained turnover of the catalyst, we can expect some loss of Cu^{2+} ions from the immobilized tricopper complexes, as Cu^{2+} is significantly more soluble in H_2O/CH_3OH relative to MeCN. Indeed, we observe more rapid loss of the tricopper complex from the MSNs when we simply turn over the catalyst by H_2O_2 in the absence of CH_4. In the latter experiment, the catalyst can only undergo abortive cycling, with 2 molecules of H_2O produced per cycle.[26,27] Consistent with this scenario, we find that the loss of the tricopper complexes from the nanoparticles to be correlated with the number of the turnover cycles, namely, with the total amounts of H_2O_2 added to the MSNs, but not with the concentrations of H_2O_2 or the durations of exposures of the MSNs to the H_2O_2.

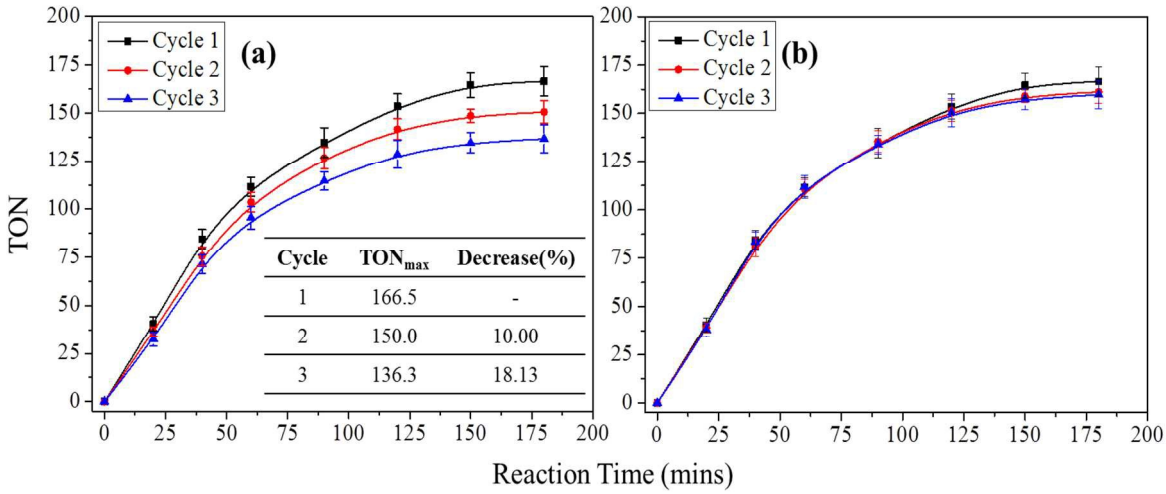

Cycle	TON_{max}	Decrease(%)
1	166.5	-
2	150.0	10.00
3	136.3	18.13

Fig. 5. (**a**) TONs of the CH_3OH obtained from the CH_4 oxidation reaction catalyzed by the **CuEtp**@AlMSN30-ex formulation at room temperature with 200 equiv. of H_2O_2 for three cycles at varying times. The TONs are expressed as moles of the substrate converted per mole of the Cu_3(**7-N-Etppz**) tricopper complex immobilized in the MSNs. (**b**) The TONs of CH_3OH of the three cycles was re-calculated based on the amount of the tricopper complex determined by ICP-MS and C/N elemental analysis before the reaction.

In an attempt to repair the system, 0.2 equiv. of $CuCl_2$ (based on the original complex loading) is added to the medium and incubated with the MSNs by stirring for 2 h prior to reuse of the catalyst. However, we observe only minor recovery of the catalytic activity. Thus we surmise that there is loss of the ligand supporting the tricopper complex during the cycling of the catalyst. It is possible that there is greater leaching of the tricopper complex from the MSNs as it is cycling through the $[Cu^ICu^ICu^I(\mathbf{L})]^{1+}$ and $[Cu^ICu^{II}(O)Cu^{II}](\mathbf{L})^{1+}$ oxidation states, compared with the $[Cu^{II}Cu^{II}(O)Cu^{II}](\mathbf{L})^{2+}$ complex that we examine earlier. If so, this leaching of the tricopper complex should be accentuated further with the loss of Cu^{2+} from the copper complex with sustained accumulation of H_2O/CH_3OH as the turnover progresses. The fully oxidized tricopper complex bears at least one additional positive charge so that we expect the tricopper complex to be less readily released from the mesporous silica nanoparticles. We believe that this shortcoming with our present *quasi*-heterogeneous formulation can be remedied by covalent attachment of the ligand to an organo-silica framework.

Discussion

In 2013, it was reported that the tricopper complex $[Cu^ICu^ICu^I(\mathbf{7\text{-}N\text{-}Etppz})]^{1+}$ could mediate the selective oxidation of CH_4 to CH_3OH in MeCN at room temperature.[26] When

the $Cu^{I}Cu^{I}Cu^{I}$ complex was activated by O_2 in the presence of CH_4, stoichiometric conversion of CH_4 to CH_3OH was accomplished in a few minutes. This chemistry mimicked the CH_4 oxidation observed for the $Cu^{I}Cu^{I}Cu^{I}$ tricopper-peptide complex that was constructed with a peptide derived from the segment of the PmoA alpha-helix lining the empty hydrophilic site D in the crystal structure of the pMMO from *Methylococcus capsulatus* (Bath).[26,32] This is the first demonstration of an enzyme active-site biomimic that is capable of efficient conversion of CH_4 into CH_3OH.

To accomplish multiple turnovers of the catalytic system, H_2O_2 was subsequently used to reduce the "spent" catalyst, namely, the $[Cu^{I}Cu^{II}(O)Cu^{II}(\textbf{7-N-Etppz})]^{1+}$ species formed after transfer of one of the O atoms to the CH_4 substrate from the activated tricopper catalyst, in order to regenerate the $Cu^{I}Cu^{I}Cu^{I}$ catalyst[27] (Scheme 1, *upper panel*). In this manner, the process became catalytic with multiple turnovers, and many turnovers were achieved without over-oxidation. Since the turnover frequency (TOF) of the catalyst is proportional to the concentration of H_2O_2 used to drive the catalytic system, attempts were made to enhance the performance of the system by going to higher H_2O_2 concentrations. However, it soon became apparent that the activated tricopper cluster was also readily reduced by H_2O_2 to form O_2 and H_2O, and this abortive process became competitive with the productive O-atom transfer process that converts CH_4 into CH_3OH as the H_2O_2 concentration was increased (Scheme 2, *lower panel*). Subsequently, it was determined that the limited solubility of CH_4 in the solvent (MeCN) used in the experiment contributed to this dilemma.[27]

Greater access to CH_4 would allow the catalyst to be operated at a higher H_2O_2 concentration to increase the TOF without compromising the catalytic efficiency.

However, at sufficiently high concentrations of H_2O_2, the H_2O_2 will also compete with O_2 in the system in the activation of the $Cu^ICu^ICu^I$ complex.[27] It turns out the $Cu^ICu^ICu^I$ tricopper cluster can also be activated by two molecules of H_2O_2.[52] With the two additional H_2O_2 molecules consumed per catalytic turnover, this scenario is accompanied by the production of two more H_2O molecules. This method of activating the tricopper complex is wasteful of H_2O_2, even though the same hydrocarbon oxidation chemistry is accomplished. To overcome some of these difficulties, it is in principle possible to operate the catalytic system under higher pressures of the CH_4 and O_2 gases, or resort to biphasic catalysis.[53] However, a simpler alternative would be to immobilize the tricopper catalyst in MSNs that are capable of sustaining high local concentrations of both CH_4 and O_2 dissolved in the mesopores/nanopores of the nanoparticles.[39-47] Here, we are exploiting the phenomenon of "over-solubility" in confined liquids to strikingly increase the solubility of a gas in the solvent confined in nanoporous materials relative to that predicted by Henry's constant for bulk solvents. Several groups have recently reported dramatic enhancements (up to 1000 folds) of hydrogen, N_2, CH_4 and other light hydrocarbons, and CO_2 solubility in solvents confined in mesoporous solids.[40,41,47]

With this *quasi*-heterogeneous catalytic system, the tricopper cluster catalyst would be activated by dissolved O_2 within the mesopores/nanopores and the molecule of H_2O_2 needed to drive the turnover would be confined to the supporting solution and only become accessible to the catalyst by diffusion to the surface of the nanoparticles. The much enhanced local concentration of CH_4 would make the productive cycle much more competitive against the abortive cycle in the catalytic turnover. This is precisely what we have achieved in this study.

With our heterogeneous catalytic system, the overall net reaction mediated by the $Cu^ICu^ICu^I$ complex is $CH_4 + H_2O_2 \rightarrow CH_3OH + H_2O$, as there is no net consumption of O_2. The disadvantage, of course, is that H_2O_2 is significantly more expensive compared to O_2 or air. However, to operate the system as a monooxgenase, a source of reductant is required to regenerate the catalyst in any case. In a methane monooxygenase, the enzyme is turned over with NADH so that the overall reaction is $CH_4 + O_2 + NADH + H^+ \rightarrow CH_3OH + NAD^+ + H_2O$. Under standard conditions of temperature and pressure, the standard free energy changes (ΔG) for the two reactions

(1) CH_4 (g) + O_2 (g) + NADH (1 M solution, pH 7) + H^+ (pH 7)

$\rightarrow$ CH_3OH (l) + NAD^+ (1 M solution, pH 7) + H_2O (l),

and

(2) CH_4 (g) + H_2O_2 (pure liquid or 35% solution) $\rightarrow$ CH_3OH (l) + H_2O (l),

are −335.1 kJ/mol and −232.8 kJ/mol, respectively, and the corresponding standard enthalpy changes (ΔH) are −423.2 kJ/mol and −262.6 kJ/mol, respectively.[54] Not surprisingly, the cellular CH_4 oxidation is almost 50% more exergonic and the monooxygenase reaction also releases 60% more heat, compared to the direct oxidation of CH_4 to CH_3OH by H_2O_2. Thus, the latter reaction is simpler and more atom and energy efficient.

Conclusion

In this study, we have shown how to significantly improve the performance of the trinuclear copper catalyst for conversion of CH_4 into CH_3OH under ambient conditions by immobilizing the tricopper complex in mesoporous silica nanoparticles. With this

formulation of the catalyst, it is possible to materially enhance the solubility of CH_4 (and O_2 as well) inside the mesopores/nanopores of the MSNs. During turnover to oxidize the CH_4, the $Cu^ICu^ICu^I$, tricopper cluster is activated by O_2, and the catalyst is regenerated by H_2O_2. In this manner, we can drive the conversion of CH_4 into CH_3OH with H_2O_2 with a catalytic efficiency approaching 100%, as well as with high energy and atom economy. It is significant that the CH_4 oxidation is proceeding with multiple or continuous complete catalytic turnover of the tricopper complex (until all the CH_4 available to the catalyst or the H_2O_2 driving the catalysis is consumed, whichever is lower), and not by a single stoichiometric turnover.[23] In principle the process can be operated at higher H_2O_2 concentrations to bolster the TOF of the catalyst, but the catalytic efficiency will be compromised. However, there are other methods to regenerate the catalyst, perhaps, with greater efficiency, and we are presently exploring the possibility of these alternatives.

Acknowledgement

This work is supported by Academia Sinica, the National Synchroton Radiation Research Center, funds from the Nanoscience and Nanotechnology Program of Academia Sinica and grants from the Ministry of Science and Technology of the Republic of China (National Nanotechnology Project NSC 100-2120-M-002-001 to CYM and MOST 101-2113-M-001-007-MY3 to SSFY).

References

1. J. A. Labinger and J. E. Bercaw, *Nature*, 2002, **417**, 507–514.
2. M. Bertau, H. Offermanns, L. Plass, F. Schmidt and H.-J. Wernicke, *Methanol: The Basic Chemical and Energy Feedstock of the Future*, Springer, Berlin/Heidelberg, 2014
3. G. A. Olah, *Angew. Chem. Int. Ed.*, 2005, **44**, 2636–2639.
4. National Academy of Engineering. *The Hydrogen Economy: Opportunities, Costs, Barriers, and R&D needs*, The National Academies Press, Washington D.C., 2004.
5. G. A. Olah, A. Goeppert and G. K. S. Prakash, *J. Org. Chem.*, 2009, **74**, 487-498.

6. R. A. Kerr, *Science*, 2010, **328**, 1624–1626.
7. D. Malakoff, *Science*, 2014, **344**, 1464–1467.
8. R. A. Periana, D. J. Taube, S. Gamble, H. Taube, T. Satoh and H. Fujii, *Science*, 1998, **280**, 560–564.
9. R. Palkovits, M. Antonietti, P. Kuhn, A. Thomas and F. Schuth, *Angew. Chem. Int. Ed.*, 2009, **48**, 6909–6912.
10. M. Soorholtz, R. J. White, T. Zimmermann, M.-M. Titirici, M. Antonietti, R. Palkovits and F. Schüth, *Chem. Commun.*, 2013, **49**, 240–242.
11. R. A. Periana, D. J. Taube, E. R. Evitt, D. G. Loffler, P. R. Wentrcek, G. Voss and T. Masuda, *Science*, 1993, **259**, 340–343.
12. P. J. Smeets, J. S. Woertink, B. F. Sels, E. I. Solomon and R. A. Schoonheydt, *Inorg. Chem.*, 2010, **49**, 3573–3583.
13. J. S. Woertink, P. J. Smeets, M. H. Groothaert, M. A. Vance, B. F. Sels, R. A. Schoonheydt and E. I. Solomon, *Proc. Natl. Acad. Sci. USA*, 2009, **106**, 18908–18913.
14. P. J. Smeets, R. G. Hadt, J. S. Woertink, P. Vanelderen, R. A. Schoonheydt, B. F. Sels and E. I. Solomon, *J. Am. Chem. Soc.*, 2010, **132**, 14736–14738.
15. P. Vanelderen, J. Vancauwenbergh, B. F. Sels and R. A. Schoonheydt, *Coord. Chem. Rev.*, 2013, **257**, 483–494.
16. E. V. Starokon, M. V. Parfenov, L. V. Pirutko, S. I. Abornev and G. I. Panov, *J. Phys. Chem. C*, 2011, **115**, 2155–2161.
17. C. Hammond, M. M. Forde, M. H. Ab Rahim, A. Thetford, Q. He, R. L. Jenkins, N. Dimitratos, J. A. Lopez-Sanchez, N. F. Dummer, D. M. Murphy, A. F. Carley, S. H. Taylor, D. J. Willock, E. E. Stangland, J. Kang, H. Hagen, C. J. Kiely and G. J. Hutchings, *Angew. Chem. Int. Ed.*, 2012, **51**, 5129–5133.
18. C. Hammond, R. L. Jenkins, N. Dimitratos, J. A. Lopez-Sanchez, M. H. Ab Rahim, M. M. Forde, A. Thetford, D. M. Murphy, H. Hagen, E. E. Stangland, J. M. Moulijn, S. H. Taylor, D. J. Willock and G. J. Hutchings, *Chem. Eur. J.*, 2012, **18**, 15735–15745.
19. E. M. Alayon, M. Nachtegaal, M. Ranocchiari and J. A. van Bokhoven, *Chem. Commun.*, 2012, **48**, 404–406.
20. E. M. C. Alayon, M. Nachtegaal, E. Kleymenov and J. A. van Bokhoven, *Microporous Mesoporous Mater.*, 2013, **166**, 131–136.
21. P. J. Smeets, M. H. Groothaert and R. A. Schoonheydt, *Catal. Today*, 2005, **110**, 303–309.
22. M. H. Groothaert, P. J. Smeets, B. F. Sels, P. A. Jacobs and R. A. Schoonheydt, *J. Am. Chem. Soc.*, 2005, **127**, 1394–1395.
23. S. Grundner, M. A. C. Markovits, G. Li, M. Tromp, E. A. Pidko, E. J. M. Hensen, A. Jentys, M. Sanchez-Sanchez and J. A. Lercher, *Nat. Commun*, 2015, **6**, doi: 10.1038/ncomms8546.
24. N. Dietl, M. Schlangen and H. Schwarz, *Angew. Chem. Int. Ed.*, 2012, **51**, 5544–5555.
25. H. Schwarz, *Isr. J. Chem.*, 2014, **54**, 1413–1431.
26. S. I. Chan, Y.-J. Lu, P. Nagababu, S. Maji, M.-C. Hung, M. M. Lee, I. J. Hsu, P. D. Minh, J. C. H. Lai, K. Y. Ng, S. Ramalingam, S. S. F. Yu and M. K. Chan, *Angew. Chem. Int. Ed.*, 2013, **52**, 3731–3735.
27. P. Nagababu, S. S.-F. Yu, S. Maji, R. Ramu and S. I. Chan, *Catal. Sci. Technol.*, 2014, **4**, 930–935.
28. S. I. Chan, K. H.-C. Chen, S. S.-F. Yu, C.-L. Chen and S. S.-J. Kuo, *Biochemistry*,

2004, **43**, 4421–4430.
29. S. I. Chan and S. S.-F. Yu, *Acc. Chem. Res.*, 2008, **41**, 969–979.
30. P. P.-Y. Chen, P. Nagababu, S. S.-F. Yu and S. I. Chan, *ChemCatChem*, 2014, **6**, 429–437.
31. S. Maji, S. S.-F. Yu and S. I. Chan, *Metalloproteins: Theory, Calculations, and Experiments*, ed. A. E. Cho and W. A. Goddard III, CRC Press, Boca Raton, 2015, ch. 4, pp.117–164.
32. R. L. Lieberman and A. C. Rosenzweig, *Nature*, 2005, **434**, 177–182.
33. P. P.-Y. Chen, R. B.-G. Yang, J. C.-M. Lee and S. I. Chan, *Proc. Natl. Acad. Sci. USA*, 2007, **104**, 14570-14575.
34. S. Maji, J. C.-M. Lee, Y.-J. Lu, C.-L. Chen, M.-C. Hung, P. P.-Y. Chen, S. S.-F. Yu and S. I. Chan, *Chem. Eur. J.*, 2012, **18**, 3955–3968.
35. S.-T. Wong, C.-H. Lee, T.-S. Lin and C.-Y. Mou, *J. Catal.*, 2004, **228**, 1–11.
36. C.-H. Lee, S.-T. Wong, T.-S. Lin and C.-Y. Mou, *J. Phys. Chem. B*, 2005, **109**, 775–784.
37. Y.-C. Fang, H.-C. Lin, I.-J. Hsu, T.-S. Lin and C.-Y. Mou, *J. Phys. Chem. C*, 2011, **115**, 20639–20652.
38. C.-H. Lee, L.-W. Lo, C.-Y. Mou and C.-S. Yang, *Adv. Funct. Mater.*, 2008, **18**, 3283–3292.
39. A. Luzar and D. Bratko, *J. Phys. Chem. B*, 2005, **109**, 22545–22552.
40. S. Miachon, V. V. Syakaev, A. Rakhmatullin, M. Pera-Titus, S. Caldarelli and J.-A. Dalmon, *ChemPhysChem.,* 2008, **9**, 78–82.
41. V. Rakotovao, R. Ammar, S. Miachon and M. Pera-Titus, *Chem. Phys. Lett*., 2010, **485**, 299–303.
42. H. Ngoc Linh, J. Perez-Pellitero, F. Porcheron and R. J. M. Pellenq, *J. Phys. Chem. C,* 2012, **116**, 3600–3607.
43. E. Soubeyrand-Lenoir, C. Vagner, J. W. Yoon, P. Bazin, F. Ragon, Y. K. Hwang, C. Serre, J.-S. Chang and P. L. Llewellyn, *J. Am. Chem. Soc.,* 2012, **134**, 10174–10181.
44. H. Linh Ngoc, S. Clauzier, Y. Schuurman, D. Farrusseng and B. Coasne, *J. Phys. Chem. Lett.*, 2013, **4**, 2274–2278.
45. H. Linh Ngoc, Y. Schuurman, D. Farrusseng and B. Coasne, *J. Phys. Chem. C*, 2015, **119**, 21547–21554.
46. A. Phan, D. R. Cole and A. Striolo, *J. Phys. Chem. C*, 2014, **118**, 4860–4868.
47. L. N. Ho, Y. Schuurman, D. Farrusseng and B. Coasne, *J. Phys. Chem.* C, 2015, **119**, 21547–21554.
48. P. Nagababu, S. Maji, M. P. Kumar, P. P. Y. Chen, S. S. F. Yu and S. I. Chan, *Adv. Synth. Catal.*, 2012, **354**, 3275–3282.
49. K.-C. Kao and C.-Y. Mou, *Microporous Mesoporous Mater.*, 2013, **169**, 7–15.
50. C.-C. Liu, T.-S. Lin, S. I. Chan and C.-Y. Mou, *J. Catal.*, 2015, **322**, 139–151.
51. S.-H. Hung, C.-L. Chen, K. H.-C. Chen, S. S.-F. Yu and S. I. Chan, *J. Chin. Chem. Soc*., 2004, **51**, 1229–1244.
52. S. I. Chan, C. Y. C. Chien, C. S. C. Yu, P. Nagababu, S. Maji and P. P. Y. Chen, *J. Catal.*, 2012, **293**, 186–194.
53. J.-M. Vincent, A. Rabion, V. K. Yachandra and R. H. Fish, *Angew. Chem. Int. Ed. Engl.*, 1997, **36**, 2346–2349.

54. *CRC Handbook of Chemistry and Physics*, ed. W. M. Haynes and D. R. Lide, CRC Press, Boca Raton, 92nd edn., 2011.

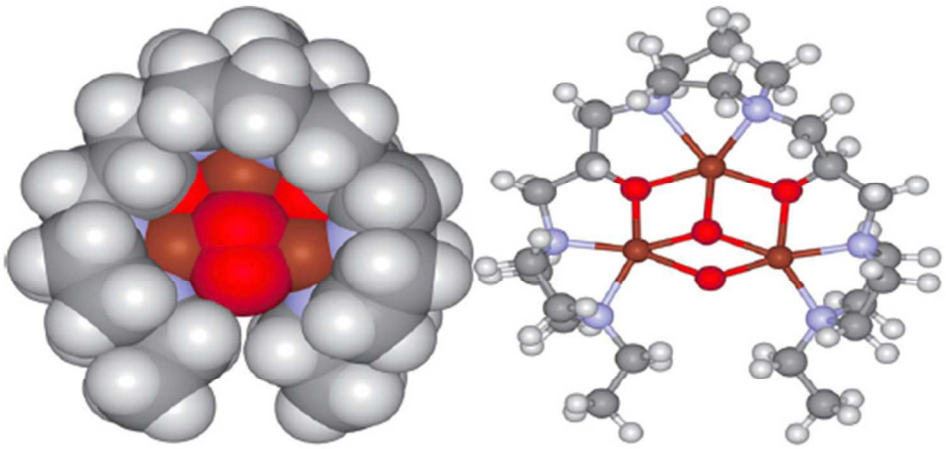

204x100mm (150 x 150 DPI)

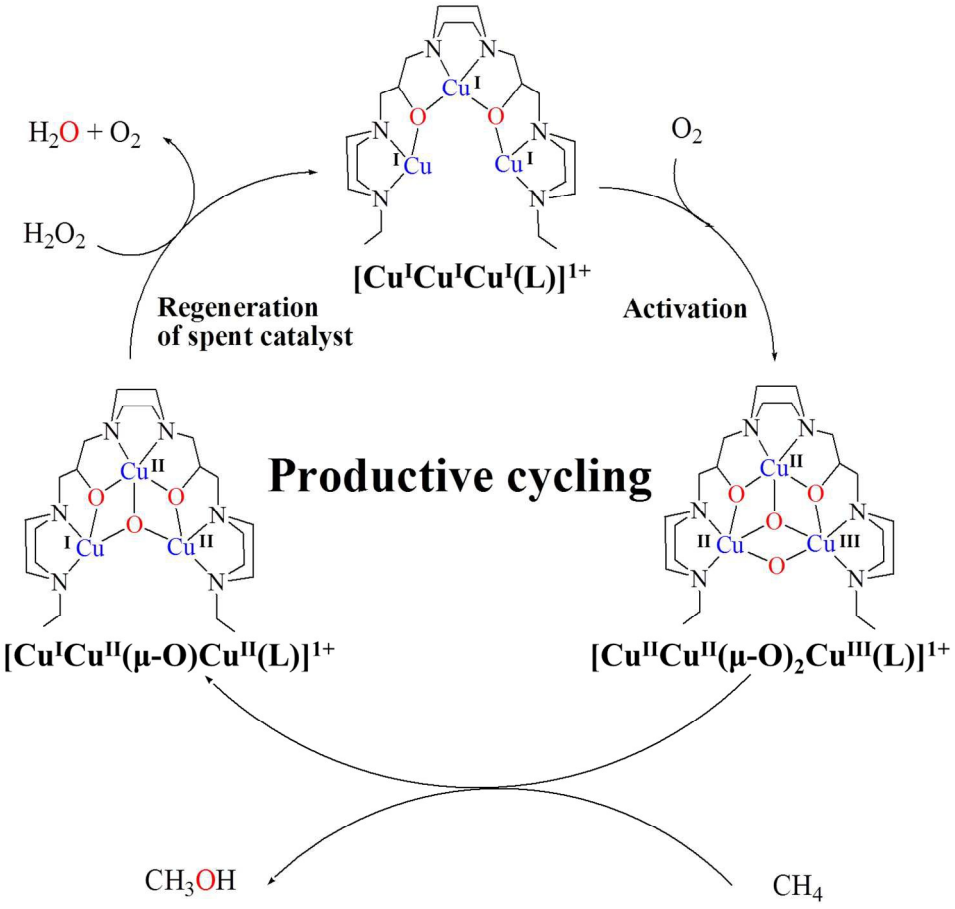

260x246mm (150 x 150 DPI)

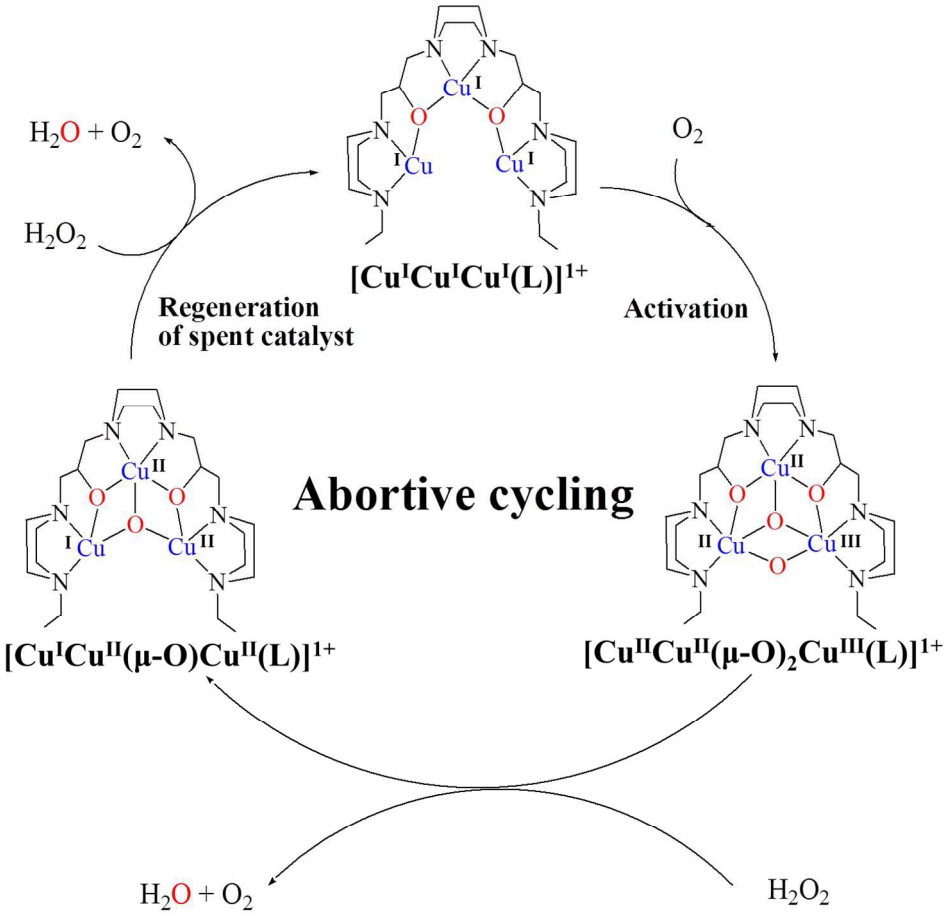

260x246mm (150 x 150 DPI)

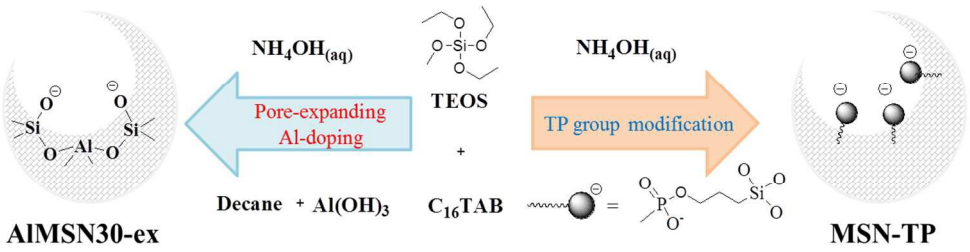

230x68mm (150 x 150 DPI)

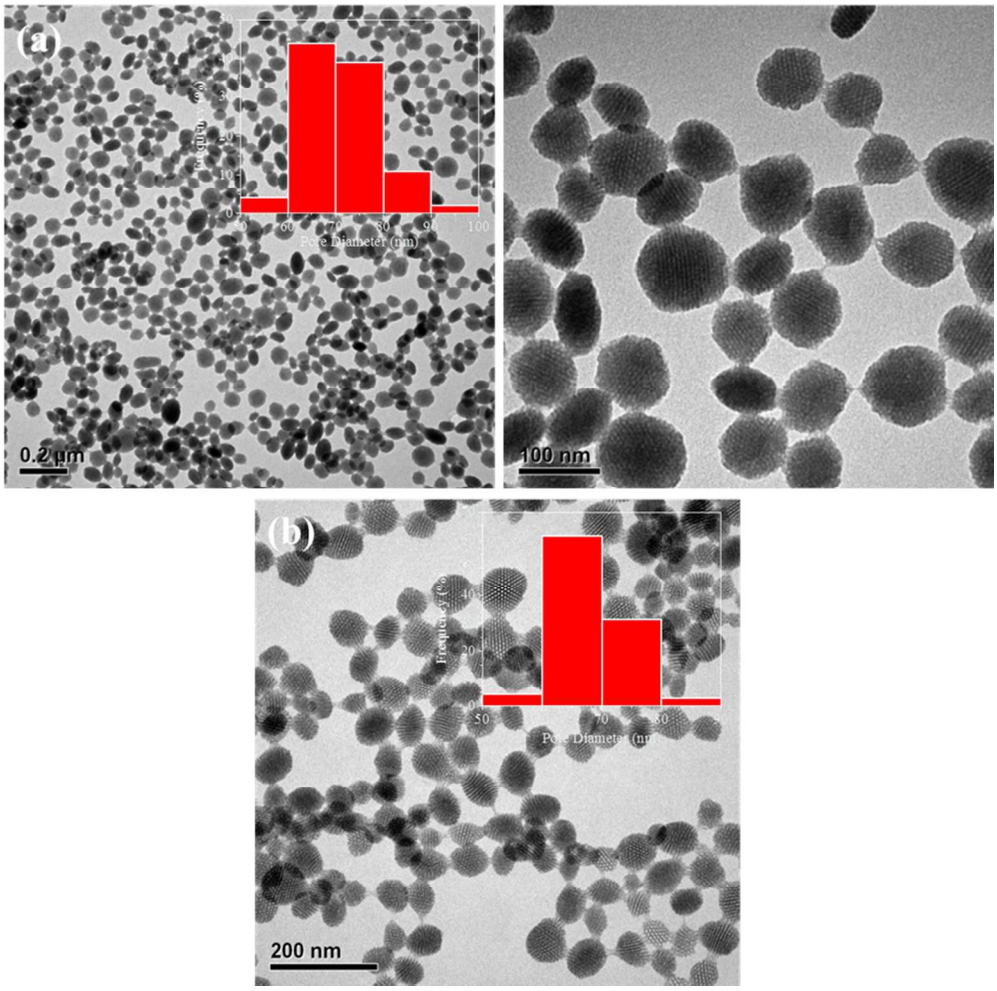

161x160mm (150 x 150 DPI)

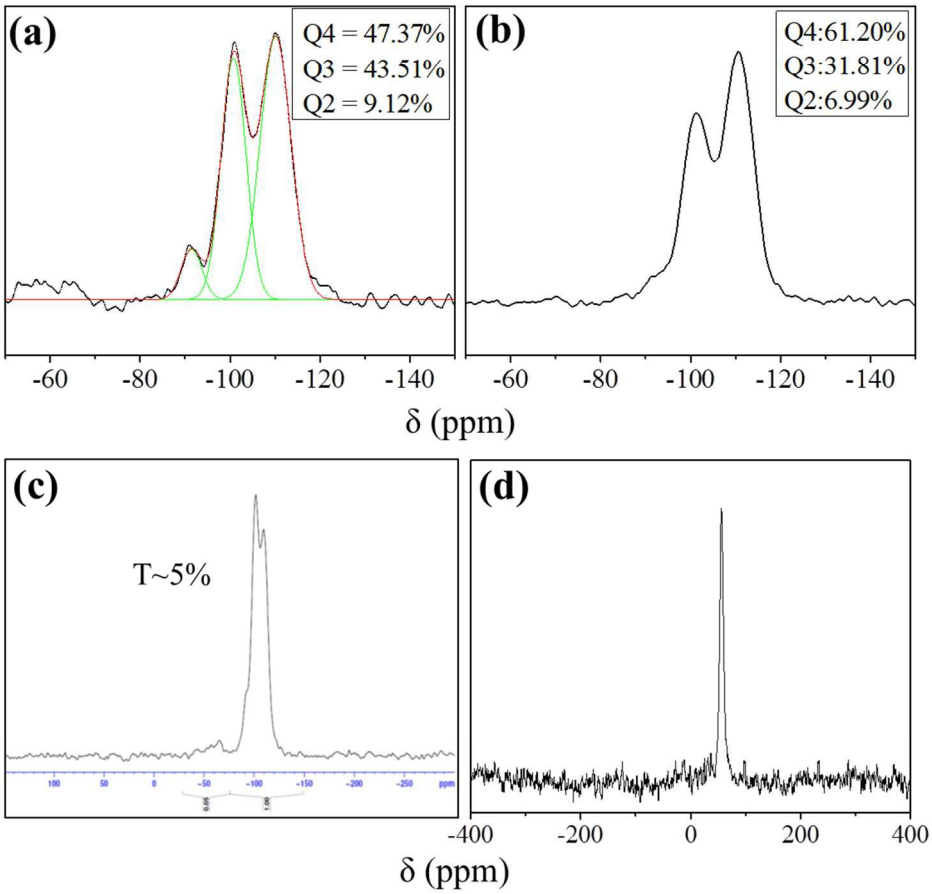

204x197mm (150 x 150 DPI)

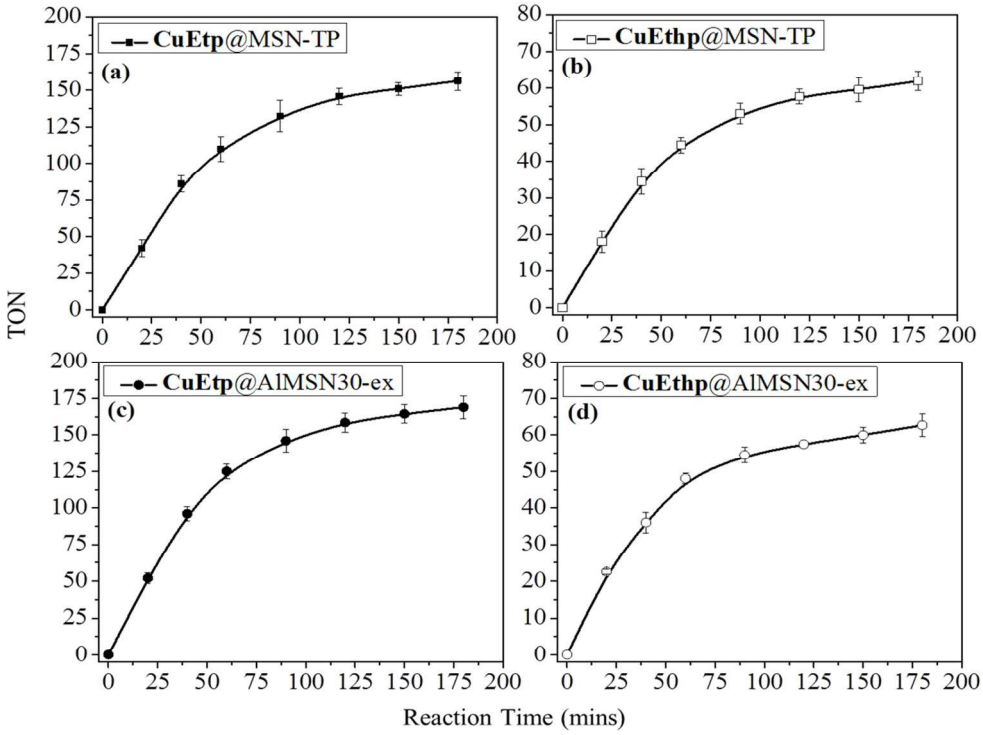

249x189mm (150 x 150 DPI)

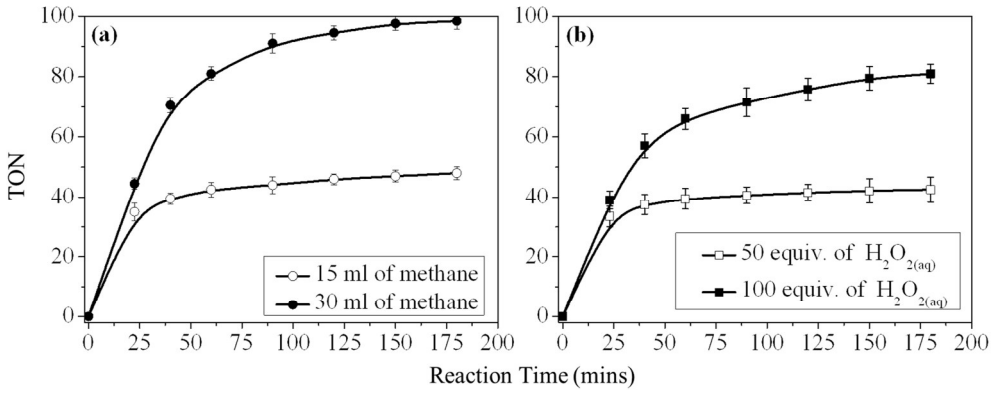

300x122mm (150 x 150 DPI)

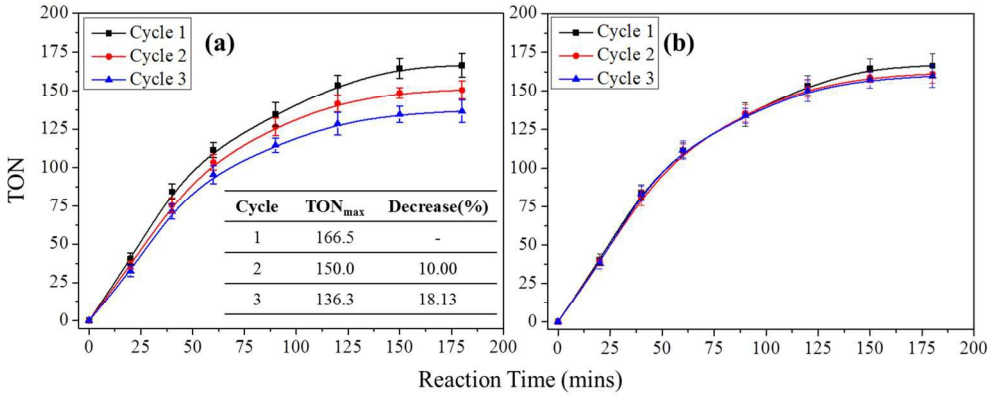

272x112mm (150 x 150 DPI)

Sample Name	Surface Area (m^2/g)	Pore Volume (cm^3/g)	Pore Diameter (nm)	Complex Adsorption (μmol/g)	zeta-potential (ζ) (mv)	
					ζ (mv)	$^a\Delta\zeta$ (mv)
MSN-TP	912.4	0.71	2.8	-	−36.2	-
CuEtp@MSN-TP	701.9	0.39	1.7	114	−22.6	+13.6
CuEthp@MSN-TP	742.2	0.41	1.8	103	−24.0	+12.2
AlMSN30-ex	1242.1	1.43	4.8	-	−46.1	-
CuEtp@AlMSN30-ex	758.9	0.90	2.6	204	−14.9	+31.2
CuEthp@AlMSN30-ex	803.9	0.93	2.8	184	−18.3	+27.8

224x87mm (150 x 150 DPI)

Sample	[a] µmol of Cu per gram of sample	[b] µmol of ligand per gram of sample	Cu / ligand ratio
CuEtp@MSN-TP	345.2	113.8	3.03
CuEthp@MSN-TP	310.1	102.6	3.02
CuEtp@AlMSN30-ex	612.9	203.6	3.01
CuEthp@AlMSN30-ex	556.3	183.6	3.03

178x89mm (150 x 150 DPI)

Cu_3(7-N-Etppz)			CuEtp@AlMSN30-ex		
Homogeneous			Heterogeneous		
H_2O_2 (equiv.)	TON_{CH3OH}	[a]OCE	H_2O_2 (equiv.)	TON_{CH3OH}	[a]OCE
0	1	-	0	1.0	-
20	6.5	0.33	20	15.9	0.80
40	~0	~0	50	42.5	0.85
100	~0	~0	100	81.1	0.81
180	~0	~0	200	171.2	0.86

232x65mm (150 x 150 DPI)

Sample Name	100 equiv. $H_2O_{2(aq)}$			200 equiv. $H_2O_{2(aq)}$		
	[b]TON	[c]Conversion	[d]OCE	[b]TON	[c]Conversion	[d]OCE
CuEtp@AlMSN30-ex	81.1	8.23	0.81	171.2	17.4	0.86
CuEthp@AlMSN30-ex	24.4	2.23	0.24	63.3	5.79	0.32
CuEtp@MSN-TP	78.4	4.44	0.78	156.5	8.87	0.78
CuEthp@MSN-TP	19.6	1.00	0.20	60.5	3.10	0.30

254x75mm (150 x 150 DPI)

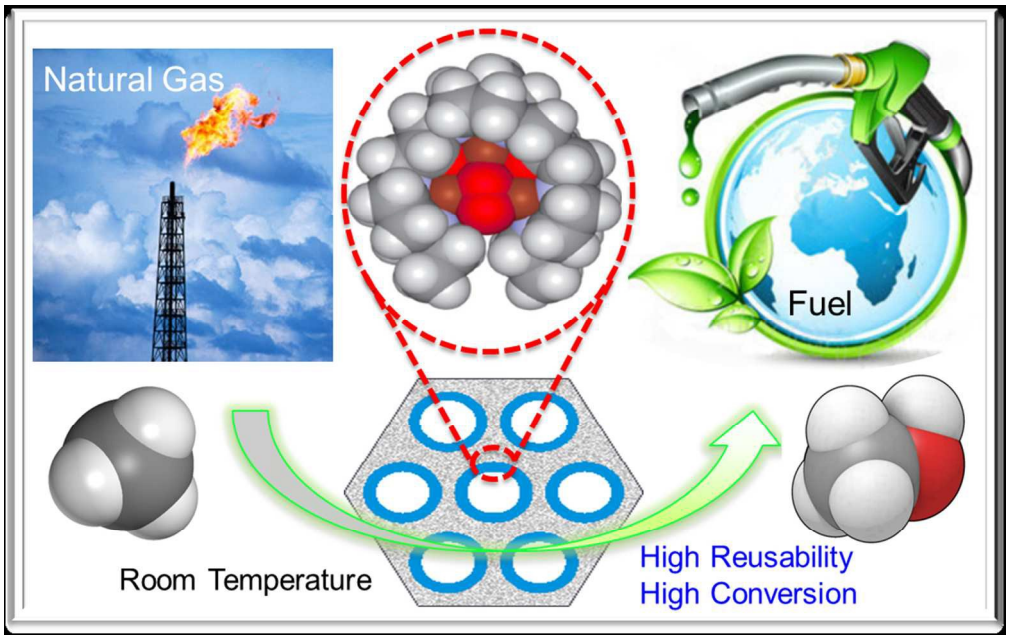

187x117mm (150 x 150 DPI)

Supplementary Information

for

Heterogeneous formulation of the tricopper complex for efficient catalytic conversion of methane into methanol under ambient temperature and pressure

Chih-Cheng Liu,[ab] Chung-Yuan Mou,[a] Steve S.-F. Yu,[b] and Sunney I. Chan*[ab]

[a] Department of Chemistry, National Taiwan University, Taipei 10617, Taiwan. Email: *cymou@ntu.edu.tw; d98223115@ntu.edu.tw*

[b] Institute of Chemistry, Academia Sinica, Nankang, Taipei 11529, Taiwan. Email: *sfyu@gate.sinica,edu.tw; sunneychan@yahoo.com*

Table of contents

A. Synthesis of ligands and preparation of tricopper complexes

Preparation of 3,3'-[1,4-diazepane-1,4-diyl]bis(1-chloropropan-2-ol) (1). A solution of epichlorohydrin (1.85 g, 20 mmol) dissolved in methanol (15.0 ml) was added drop-wise to a solution of homopiperazine (1.02 g, 10 mmol) dissolved in methanol (30.0 ml) and stirred at 5 °C. After stirring for 72 h at 5 °C, the resulting mixture was purified by column chromatography on silica gel using a mixed solvent (8% CH_3OH in CH_2Cl_2) as the eluent. Compound **1** was obtained in 88% yield (2.50 g).

Synthesis of the ligand (3,3'-(1,4-diazepane-1,4-diyl)bis[1-(4-ethylpiperazine-1-yl) propan-2-ol]) (7-N-Etppz). K_2CO_3 (4.15 g, 30 mmol) was added to a CH_3CN (15.0 ml) solution containing compound **1** (4.28 g, 15 mmol), and 1-ethylpiperazine (3.46 g, 30 mmol). The mixture was then heated to 70-80 °C for 48 h under a N_2 atmosphere. After cooling to room temperature, the solution was filtered, and upon evaporation of the filtrate to dryness, the ligand **7-N-Etppz** was obtained. ^{1}H NMR ($CDCl_3$, 300 MHz): 1.8 (t, 2H, CH_3); 2.05-2.93 (m, CH_2); 3.6 (s, 2H, CH), 4.4 (s 2H, CH). ^{13}C NMR (300 MHz, $CDCl_3$): the major peaks appeared at 11.74, 11.82, 27.10, 52.0, 52.5, 53.2, 54.4, 55.3, 62.2, 62.4, and 64.7. The ESI-MS (positive ion): m/z 441.

Synthesis of the ligand (3,3'-(1,4-diazepane-1,4-diyl)bis[1-(4-ethylhomopiperazine -1-yl)propan-2-ol]) (7-N-Ethppz). Following the same procedure as above, **7-N-Ethppz** was prepared by mixing compound **1** (4.29 g, 15 mmol) with 1-ethylhomopiperazine (3.80 g, 30 mmol). Yield: 80% (5.6 g). ^{1}H NMR ($CDCl_3$, 300 MHz): 1.11 (s, 4H, CH_3), 1.14 (m, 4H CH_2), 1.15 (d, 6H, CH_2), (m, 16H, CH_2), 2.41-2.88 (m, 8H, CH_2), 3.13 (d, 2H, CH). ^{13}C NMR (300 MHz, $CDCl_3$): 12.2, 25.4, 46.2, 52.3, 52.5, 52.7, 54.2, 62.0 and 65.5. The ESI-MS (positive ion): m/z 469.

Preparation of the $Cu^{II}Cu^{II}Cu^{II}$ tricopper complex, Cu_3(7-N-Etppz). A anhydrous CH_3CN solution (25 ml) containing **7-N-Etppz** (2.205 g, 5.0 mmol) and three equivalents of $Cu^{II}(ClO_4)_2 \cdot 6H_2O$ (5.49 g, 15.1 mmol) were mixed and stirred for 1 h to give a deep green solution, which was filtered, washed with CH_2Cl_2, and dried in vacuum to give a green powder. The calculated yield was 4.00 g (95%). The elemental analysis of $C_{23}H_{46}O_{11}N_6Cl_2Cu_3$ gave C, 32.77; H, 5.50; N, 9.94%, which were the same as the calculated values within experimental uncertainty: C, 32.72; H, 5.49; N, 9.96%. The ESI-MS (positive ion): m/z 844.02.

Preparation of the $Cu^{II}Cu^{II}Cu^{II}$ tricopper complex, Cu_3(7-N-Ethppz). A anhydrous CH_3CN solution (25 ml) containing **7-N-Ethppz** (2.345 g, 5.0 mmol) and three equivalents of $Cu^{II}(ClO_4)_2 \cdot 6H_2O$ (5.49 g, 15.1 mmol) were mixed and stirred for 1 h to give a blue solution, which was filtered, washed with CH_2Cl_2, and dried in vacuum to give a blue powder. The calculated yield was 4.23 g (97%). The elemental analysis of $C_{25}H_{50}O_{11}N_6Cl_2Cu_3$ gave C, 34.48; H, 5.82; N, 9.60%, which were the same as the calculated values within experimental uncertainty: C, 34.42; H, 5.78; N, 9.63%. The ESI-MS (positive ion): m/z 872.09.

B. Supplementary Figures S1-S7

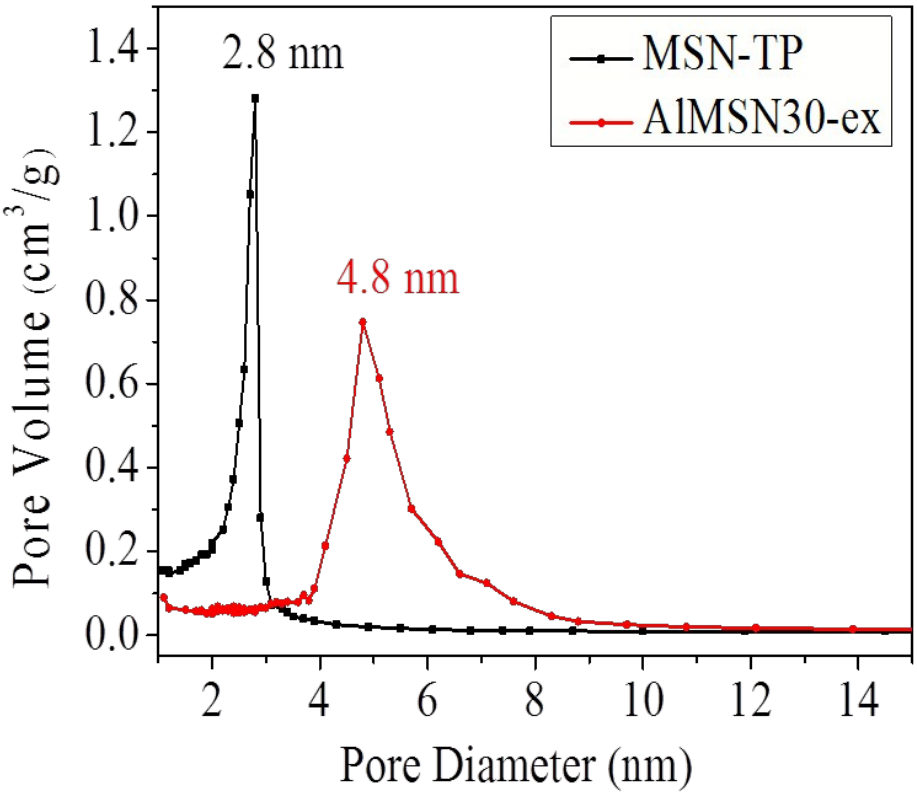

Fig. S1. Plots of the pore size distribution of the MSN-TP and AlMSN30-ex samples. The pore size is 2.8 ± 0.14 nm for the MSN-TP sample and is 4.8 ± 0.57 nm for the AlMSN30-ex sample.

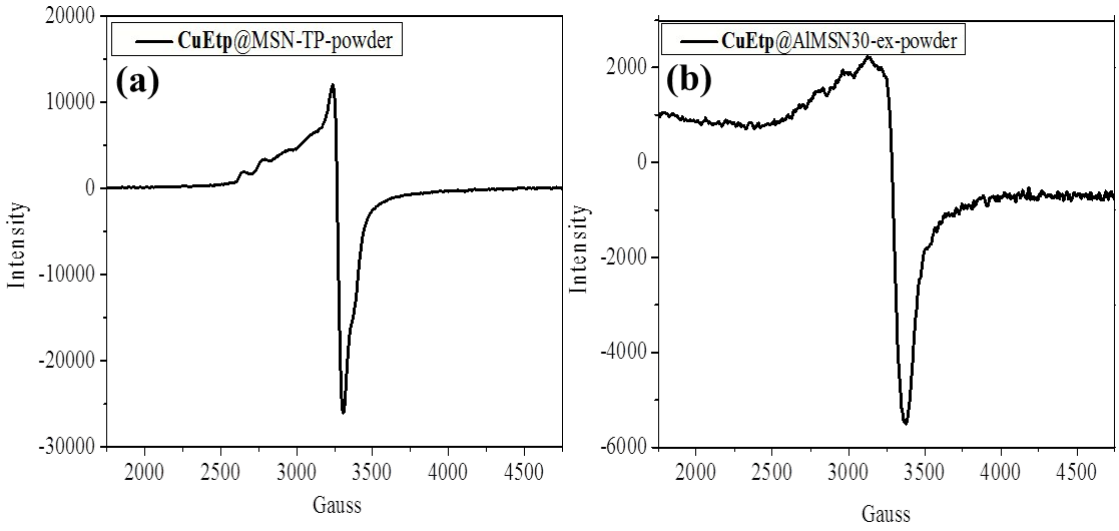

Fig. S2. X-band EPR spectra of MSN samples at 77 K: (**a**) **CuEtp**@MSN-TP; and (**b**) **CuEtp**@AlMSN30-ex. Conditions: Microwave frequency: 9.45 GHz; microwave power: 10 mW; and modulation amplitude: 8 G.

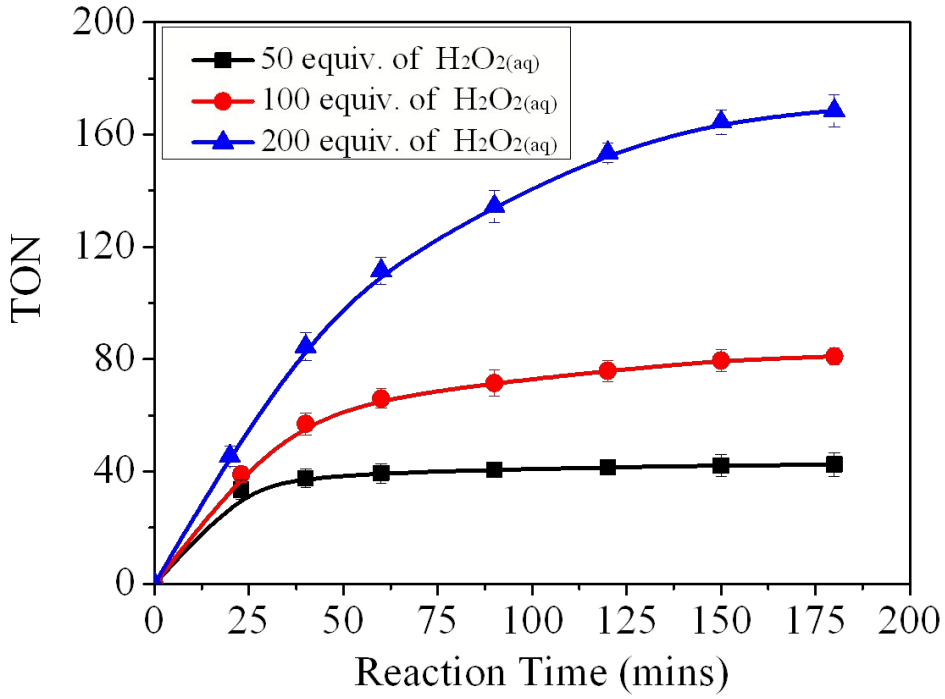

Fig. S3. Time course of the TONs for the methane oxidation reaction catalyzed by the best performing catalyst, **CuEtp**@AlMSN30-ex, at room temperature using different amounts of H_2O_2 (equiv.) to drive the catalytic turnover.

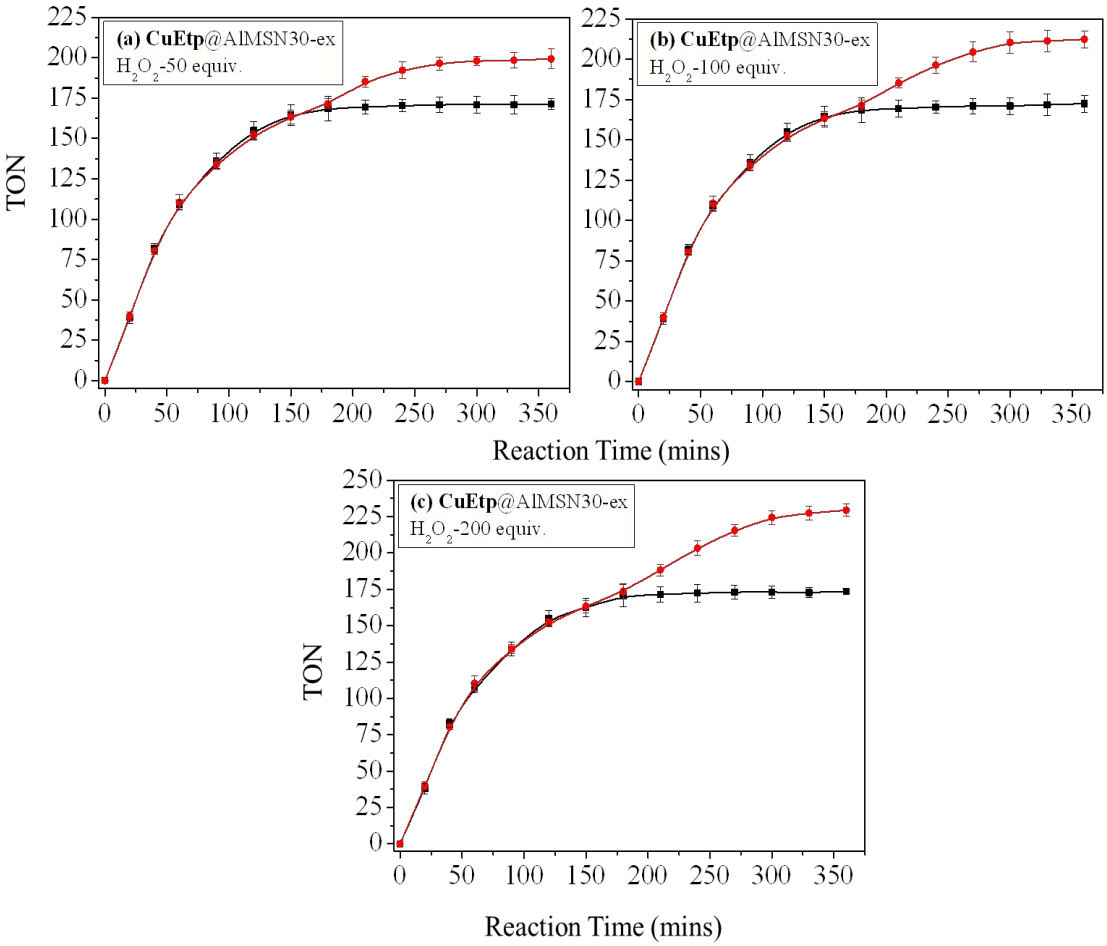

Fig. S4. Sustaining the catalytic turnover of the tricopper complex toward methane oxidation mediated by $[Cu^{I}Cu^{I}Cu^{I}(\textbf{7-N-Etppz})]^{1+}$ immobilized in the **CuEtp**@AlMSN30-ex formulation. The turnover was first initiated by 200 equiv. of H_2O_2 in the presence of 100 ml of CH_4 (986 equiv.) and 10 ml of O_2 (98.6 equiv.), and the time course of the TON for the methane oxidation reaction was monitored for 3 h at room temperature. At the end of this period, the sample was re-purged with 50 equiv. of methane and the TON monitored up to 6 h without the introduction of additional H_2O_2 (black line); or with the introduction of additional H_2O_2: (**a**) 50 equiv.; (**b**) 100 equiv.; and (**c**) 200 equiv. Adding 50 equiv. of methane (black line) did not increase the turnover number of methanol because the H_2O_2 used to initiate the original turnover had already been consumed during the first 3 h. However, further methane oxidation was observed up to 6 h with the injection of a new aliquot of H_2O_2.

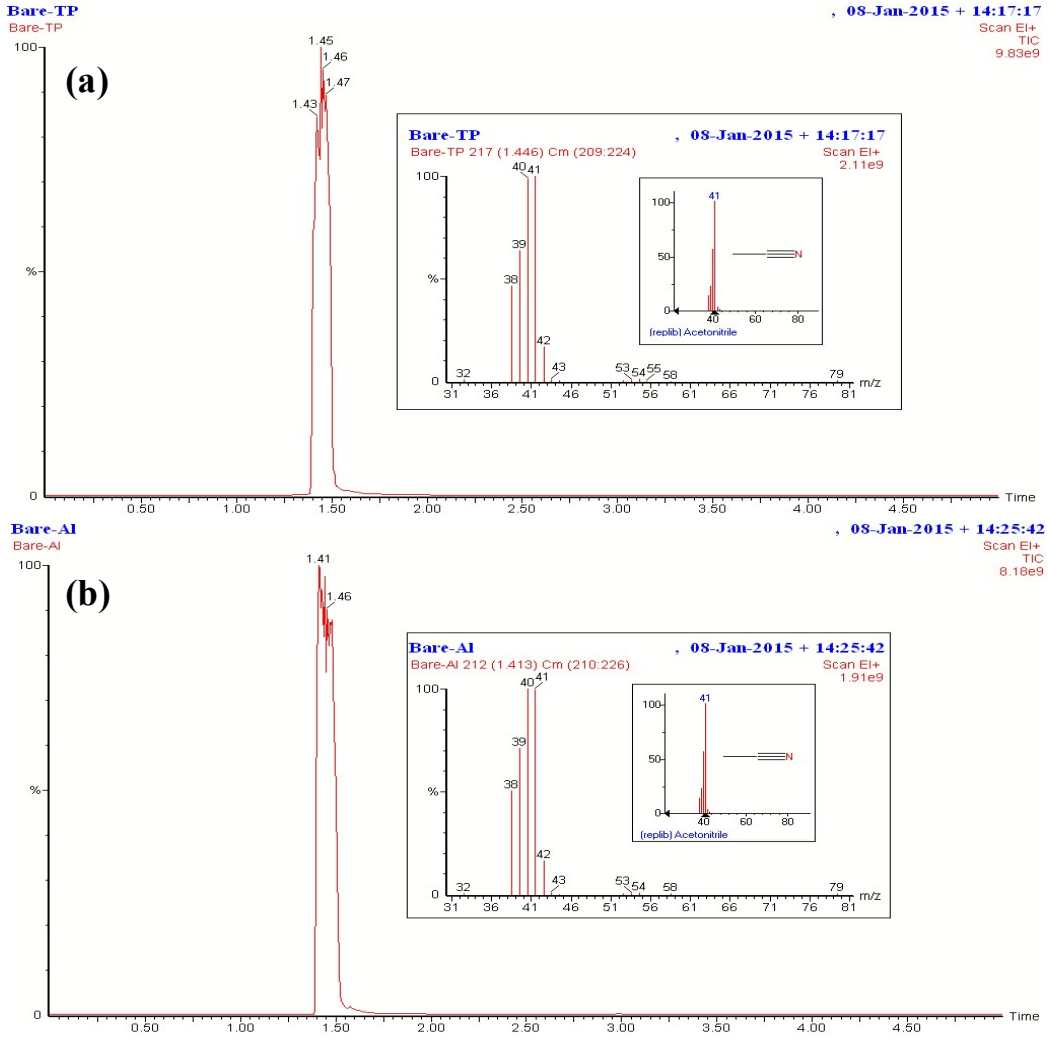

Fig. S5. GC-MS spectra of the products observed in the methane oxidation reaction attempted using the (**a**) bare MSN-TP sample, and (**b**) bare AlMSN30-ex sample, for 3 h. These control experiments were performed according to the same procedures used in the methane oxidation reaction mediated by the *quasi*-heterogeneous tricopper complex formulations. 20 mg of the bare MSN-TP or bare AlMSN30-ex samples was first suspended in O_2-free acetonitrile (5 ml) in a 50 ml Schlenk flask. The samples were then purged with O_2 (10 ml at STP, 0.44 mmol) and CH_4 (100 ml STP, 4.4 mmol). Finally, an aliquot of 200 equiv. of H_2O_2 was injected into the sample after adding the amounts of sodium ascorbate solution typically used in the methane oxidation with the tricopper complex-immobilized MSN samples. The heterogeneous mixture suspension was then stirred vigorously at room temperature for 3 h and analyzed by using GC-MS. No oxidation products were observed. *Inset*: The fitted MS spectrum from the built-in MS database software.

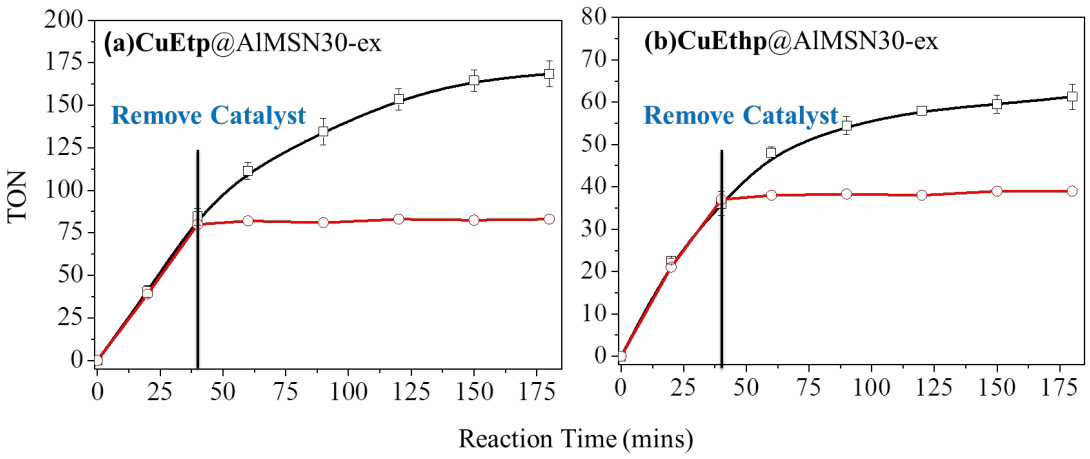

Fig. S6. Time course of the TONs for the methane oxidation reaction catalyzed by (**a**) **CuEtp**@AlMSN30-ex, and (**b**) **CuEthp**@AlMSN30-ex samples at room temperature with 200 eq. of H_2O_2 (black line). In each case, a parallel experiment was also conducted under the same conditions, except that the catalytic turnover was interrupted 40 min into the experiment to quickly separate and remove the MSNs from the liquid phase by centrifugation. Measurement of the catalytic activity was then continued on the supernatant until the end of the 3-h experiment (red line). No catalytic activity was observed for the supernatant.

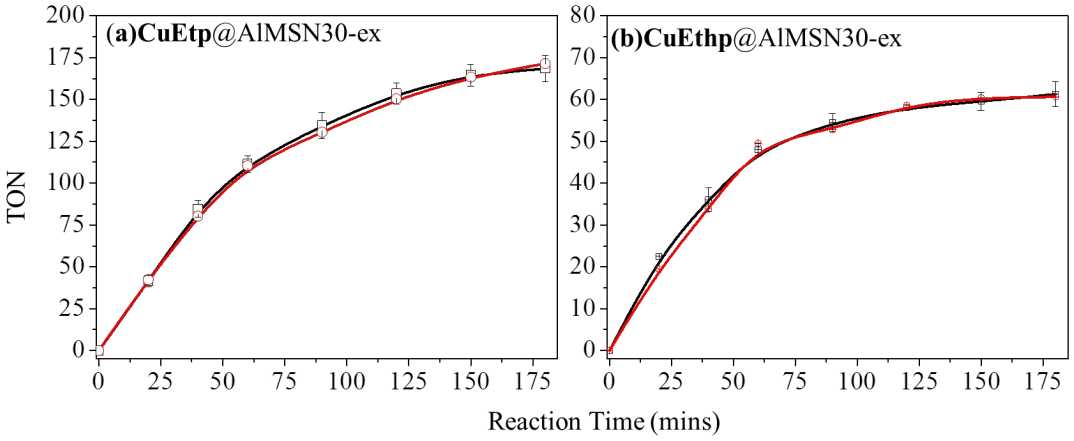

Fig. S7. Comparison of the time courses of the methane oxidation reaction mediated by (**a**) **CuEtp**@AlMSN30-ex, and (**b**) **CuEthp**@AlMSN30-ex at room temperature in the absence (black line) and presence (red line) of the radical trapping agent 2,6-di-*tert*-butyl-*p*-cresol (1 equiv., based on the amount of the immobilized tricopper complexes in the AlMSN30-ex samples). The TONs of the products are expressed in terms of the moles of product formed per mole of the tricopper complex in each case.

Supplementary Table

Table S1. Time course of leaching of the tricopper $Cu^{II}Cu^{II}Cu^{II}$ complexes from the MSNs at 25 ^{o}C.

Sample	**CuEtp@MSN-TP**	**CuEthp@MSN-TP**	**CuEtp@AlMSN30-ex**	**CuEthp@AlMSN30-ex**
Time (h)	Released (ppm)	Released (ppm)	Released (ppm)	Released (ppm)
0	0	0	0	0
0.5	4	4	2	3
1.0	6	7	5	6
2.0	10	12	8	11
4.0	14	15	11	13
6.0	16	20	13	16
8.0	18	24	16	18
10.0	22	26	18	20